NACA RM A54J14

NACA

RESEARCH MEMORANDUM

A FLIGHT AND ANALOG COMPUTER STUDY OF SOME STABILIZATION AND COMMAND NETWORKS FOR AN AUTOMATICALLY CONTROLLED INTERCEPTOR DURING THE FINAL ATTACK PHASE

By Howard L. Turner, William C. Triplett, and John S. White

Ames Aeronautical Laboratory
Moffett Field, Calif.

NATIONAL ADVISORY COMMITTEE FOR AERONAUTICS

WASHINGTON

March 23, 1955

NACA RM A54J14

NATIONAL ADVISORY COMMITTEE FOR AERONAUTICS

RESEARCH MEMORANDUM

A FLIGHT AND ANALOG COMPUTER STUDY OF SOME STABILIZATION AND COMMAND NETWORKS FOR AN AUTOMATICALLY CONTROLLED INTERCEPTOR DURING THE FINAL ATTACK PHASE

By Howard L. Turner, William C. Triplett,
and John S. White

SUMMARY

Studies of the final attack phase of an automatically controlled interceptor were conducted in flight and on electronic simulators to investigate various airplane command and stabilization networks and to develop simple but adequate simulation techniques for the synthesis of automatic control systems. A low-speed airplane equipped with an optical radar simulator was used as the test vehicle in flight tests at one airspeed and one altitude and in various pure pursuit attack situations. A number of interesting results were found for the various airplane command and stabilization networks studied but the extent to which these can be applied to the synthesis of high-performance systems will depend on the individual situation.

Of the various automatic control systems investigated, the one which gave the most favorable compromise tracking performance for a variety of test maneuvers was essentially a rate stabilization system (pitch rate in elevation, and roll and yaw rates in azimuth). Of possible general interest was the incorporation of integrating networks in azimuth and elevation (to eradicate bias errors in turning maneuvers) and a nonlinear gain in azimuth (to permit stable but rapid reduction of both large and small azimuth errors). An automatic rudder turn coordination network was used successfully in all flight tests to maintain sideslip angles near zero.

The selection and modification of the various loops for this final system were based, in a large part, on the results of analog-computer studies. Subsequent flight tests verified the adequacy of the simulation procedures employed.

With this selected automatic control system, tracking of airborne targets was generally smoother and more precise than corresponding

manually controlled tracking. In steady straight tail-chase runs, for example, the standard deviations of the gun-line wander in azimuth and elevation under automatic control were about one mil and, under manual control, about two mils. Somewhat larger errors were experienced in transient flight conditions under automatic control than under manual control; however, they were not considered excessive.

The average radial standard deviation of the tracking-line wander of the optical radar simulator was less than one mil. The excellent tracking performance with this manually operated optical sighting device may be of interest in connection with the design of director-type fire-control systems.

INTRODUCTION

The difficulty of intercepting modern bomber aircraft has led to an increased interest in the use of automatic control equipment to improve the interceptor guidance during the final attack run and to free the pilot for the more important monitoring and judgment functions. In general, these interceptor automatic control systems are composed of three basic elements: a target detector which establishes the target location and motions with respect to the interceptor; computer elements which receive data such as target location, target relative motion, ballistic information, etc., and which furnish tracking commands to the airplane and/or the target detector; and an automatically stabilized airplane which receives maneuvering commands from the computer elements. Interceptor response and target motions form outer kinematic loops which establish the inputs to the target detector.

Such automatic interceptor control systems are complex and their performance, as indicated by the probability of kill, is influenced by many variables such as tactics, armament characteristics, radar noise, computer dynamics, interceptor aerodynamic and mass-distribution characteristics, etc. This makes it difficult to produce research results of general usefulness to designers. The present research program is restricted to one problem of general interest, the design of automatic command and stabilization systems capable of producing fast accurate interceptor response to tracking error signals. Much analytical work has been done on various aspects of the final attack phase of the automatic-interception problem, as indicated by references 1 to 5. These studies were generally limited to analytical investigations of the stabilization and command-system response characteristics or of the tracking performance in simple two-dimensional tracking problems. While such studies provide necessary information, it was felt that the present study should be extended to include, within the limitations of available equipment, analytical and flight investigations of the tracking performance of an interceptor in a variety of three-dimensional attack situations.

A low-speed, servo-equipped, two-place airplane was available for the flight-test phase of this investigation. To eliminate the complications of an airborne self-tracking target detector, a manually operated optical device was used to simulate a noise-free, lag-free, tracking radar. The tests were conducted at one airspeed and one altitude with pure pursuit tracking (no ballistic lead). Tracking inaccuracies, as measured by the angles between a fuselage reference line (gun line) and the line of sight during various attack maneuvers against airborne targets, were used as a basis for comparing the various command and stabilization systems. A high-speed electronic simulator and a Reeves Electronic Analog Computer were available for the corresponding system analysis and synthesis studies.

It is difficult to draw generalizations from this single investigation of a simplified system in a low-performance airplane. However, this investigation illustrates a technique of combined flight and simulator studies which, when applied to more complex systems in higher-performance airplanes, can lead to well-verified generalizations and design procedures. It was believed that the results of this study might serve as a guide to the initial selection of promising stabilization and command systems, and that the concurrent flight-simulator technique would facilitate development of relatively simple but adequate methods of representing the complex systems and problems on electronic simulators. This would permit rational extension of the present analysis to include such complications as radar noise and attack computers and to consider more modern airplanes and other system components of higher performance.

NOTATION

A_Z	normal acceleration, g
H	horizontal displacement (azimuth) of target from interceptor at t=0, ft
K	gain constant
K_V	integrating network gain
R	range, ft
V	velocity, ft/sec
g	acceleration due to gravity, 32.2 ft/sec^2
h	horizontal displacement (azimuth) of interceptor at t seconds, ft
p	rolling velocity, radians/sec (output of roll rate gyro in airplane coordinates)

[redacted]

q	pitching velocity, radians/sec (output of pitch rate gyro in airplane coordinates)
r	yawing velocity, radians/sec (output of yaw rate gyro in airplane coordinates)
s	Laplace operator, $\frac{d}{dt}$
t	time, sec
v	voltage
α	angle of attack, deg
$\dot{\alpha}$	rate of change of angle of attack, radians/sec
β	sideslip angle, deg
$\dot{\gamma}$	rate of change of flight path ($\dot{\gamma} = q - \dot{\alpha}$), radians/sec
δ_A	total aileron deflection, deg
$\dot{\delta}_A$	rate of change of aileron deflection, deg/sec
δ_E	elevator deflection, deg
$\dot{\delta}_E$	rate of change of elevator deflection, deg/sec
δ_R	rudder deflection, deg
$\dot{\delta}_R$	rate of change of rudder deflection, deg/sec
θ	pitch angle (from horizontal), deg (space coordinates)
$\dot{\theta}$	pitching velocity, radians/sec (space coordinates)
σ	standard deviation gun-line wander, mils
φ	roll angle, deg
ψ	yaw angle, deg (space coordinates)
$\dot{\psi}$	yawing velocity, radians/sec (space coordinates)
ϵ	gun-line error, mils
η	inclination of gun line from fuselage datum line

λ radar simulator tracking-line error, mils

λ' sighting error, mils

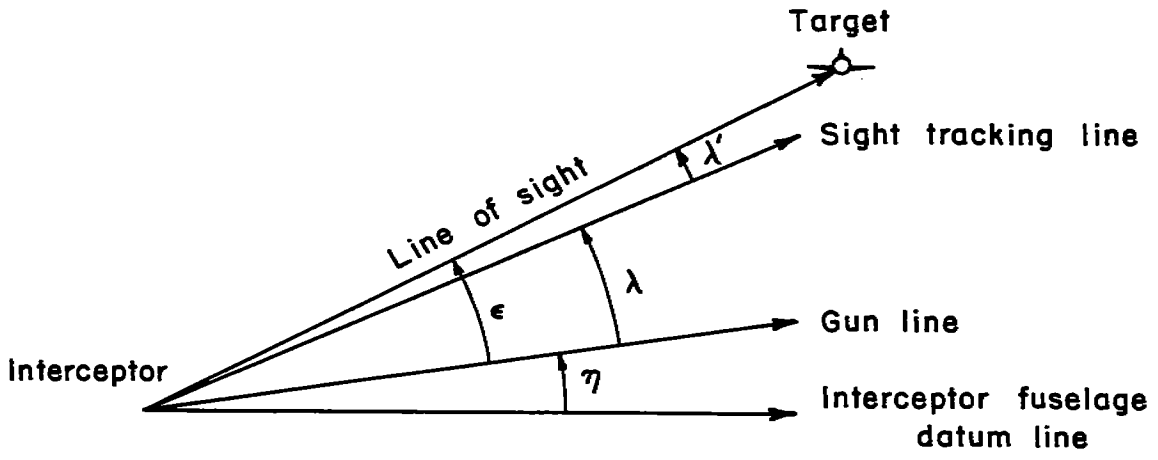

Sketch (a)

Subscripts

ψ azimuth component in space coordinates

θ elevation component in space coordinates

i input

o initial conditions at t=0, sec

ϵ error

e elevation component in airplane coordinates

a azimuth component in airplane coordinates

EQUIPMENT

Interceptor

The test vehicle used as an interceptor in this investigation was a single-engined, propeller-driver, two-place SB2C-5 Navy dive bomber modified to accommodate a manually operated optical radar simulator and equipped with electrically actuated hydraulic servos on all control surfaces. Figure 1 is a photograph of this airplane in flight. Detailed descriptions of the airplane and the servo equipment are given in references 6 to 8.

Radar Simulator

A noise-free lag-free radar was simulated by a manually operated, periscopic, sighting station which had been designed for the remote control of aircraft gun turrets. This sighting station was modified by changing the elevation gearing (degree rotation of hand control per degree line of sight) from 1:1 to 2.25:1 and by the addition of viscous damping in azimuth and elevation to improve the sight tracking characteristics. The azimuth gearing, 1° controller for 1° line of sight, was not modified. In operation, this device was manually controlled to keep the sight tracking line directed at the intersection of the horizontal and vertical tails of the target airplane. Pick-offs provided electrical signals to the automatic control system that were proportional to the azimuth and elevation angles of the sight tracking line with respect to the gun line of the interceptor, in interceptor body axes.

As shown in figure 1, this sighting station was located above and behind the front cockpit to provide the sight operator with an unobstructed field of view. The optical axis of the radar simulator, in its neutral position, was parallel to the optical axis of the Mark 8 Mod 5 gun sight in the front cockpit. This gun-sight axis represented the gun line of the interceptor. The sight axes were inclined 5° nose up with respect to the fuselage datum line, primarily to avoid the wake of the target airplane. Figure 2 is a photograph of the radar simulator.

Flight Instrumentation

Time histories of pertinent motions of the interceptor and of the control surfaces and selected voltages in the automatic control system were recorded in flight on an 18-channel Consolidated oscillograph. Two 16-mm GSAP cameras were used to photograph the target airplane, one along the axis of the interceptor gun line (through the Mark 8 Mod 5

gun sight), and one along the sight tracking line (through the radar simulator). Identification pips for each frame were recorded on the oscillograph to permit a time correlation of all recorded data. Statistical data for determining the tracking performance of the interceptor were obtained from analysis of the 16-mm film. Diagrams of the pictures obtained from the 16-mm GSAP cameras are shown in figure 3.

TESTS, RESULTS, AND DISCUSSION

As an aid in assessing the significance of the tests and results of this investigation, let us first compare briefly a representative automatic control system with the simplified automatic control system studied in this investigation. A simplified block diagram of one channel of a representative director-type automatic interceptor control system is given in figure 4(a). The target position and motions, with respect to the interceptor, are determined by an automatic tracking radar. Associated electric signals, along with other input quantities, are then fed to an attack computer which calculates and compares desired and actual angles between line of sight and the interceptor axes for some selected type of attack course (such as lead pursuit, constant bearing, etc.). Signals proportional to these angular differences, which represent airplane tracking errors, are fed as commands to the stabilized airplane.

For the present investigation, it was desirable to simplify this typical automatic control system in order to facilitate study of the gross effects of changes in the major components on the over-all tracking performance. The simplification employed is demonstrated by the basic block diagram of one channel of the automatic control system in figure 4(b). The manually operated optical device was assumed to track the target with negligible noise or other error so that its output represents the angle between the line of sight and the interceptor gun line, used as a measure of the interceptor tracking error; these signals are fed directly to the appropriate control channel of the stabilized airplane as command signals. As can be readily seen, the stabilization loops are similar in both cases, but the simplified SB2C-5 system neglects the dynamics of the radar and computers. In order to minimize the importance of these differences in the present study, airplane tracking performance has been investigated for a variety of target and interceptor conditions and target maneuvers, which approximate kinematic and interceptor automatic control problems common to all such systems. Thus, despite the simplification shown in figure 4(b), the results may serve as a guide in the synthesis of the more complicated automatic control systems as represented by figure 4(a).

The tests and results of this investigation will be discussed in the following sections in the order indicated below: (a) development of suitable stabilization and turn coordination networks and preliminary

tracking with a simple error-signal command system; (b) use of analog computers to design signal modifiers to improve the performance of this simple command system; and (c) evaluation of the tracking performance with the automatic control system developed from the combined analog-computer and flight studies.

Automatic Control With a Simple Command System

In this first phase of the investigation, it was expedient to employ a simple error-signal command system, as exemplified by figure 4(b), to facilitate the examination of the gross effects of various stabilization and turn coordination networks on the tracking performance of an automatically controlled interceptor. As discussed in detail below, the various networks were examined briefly on a limited-capacity high-speed electronic simulator to determine the gain levels required for flight and the stable regions of parameter adjustment. Flight tests were then conducted and the network gains were adjusted to give optimum response. Flight tracking studies were then conducted, using the simple command system and the optimum stabilization and turn coordination network gains, to determine the feasibility of tracking with such a simplified automatic control system.

Development of stabilization and turn coordination networks.- The first step in the present investigation was to determine suitable stabilization and turn coordination networks. To facilitate the selection of desirable feedback signals and the corresponding gain levels, a high-speed electronic simulator was used. A block diagram of the automatic control system, as studied on the simulator, is shown in figure 5 (brief tests of the gyros used in the flight tests indicated that their dynamic effects could be neglected in this simulation). The response characteristics in elevation and azimuth were determined independently by introducing a square pulse voltage (approximately 1.3 second) into the circuit at v_e and v_a, respectively. Similar tests were later conducted in flight and the flight response characteristics and gain levels which produced the best tracking results for each stabilization loop are shown in table I. For convenience, only the pitching-velocity response for the elevation channel and the yawing-velocity response for the azimuth channel are shown. Good correlation between flight and simulator results was achieved.

In order to obtain satisfactory tracking performance, θ and Ψ should reach constant steady values in the shortest possible time with no appreciable overshoot. Hence, the responses q and r should follow the shape of the square pulse inputs. On this basis it appears that for the elevation channel, stabilization loop (c) which has pitching-velocity feedback will give satisfactory tracking. Pitch-angle feedback (stabilization loop (a)) does not provide sufficient damping and will produce steady-state errors when tracking a target in steady climbing or diving flight.

[redacted]

Normal acceleration feedback (stabilization loop (d)) appears to be only marginally acceptable in the absence of shaping networks.

In the azimuth channel, the use of a rolling-velocity signal alone (stabilization loop (a)) is unsatisfactory because, in correcting an initial tracking error, maximum bank angle and maximum turning rate are reached as the error approaches zero. Bank-angle feedback (stabilization loop (b)) appears to be satisfactory; however, the addition of a roll-rate signal, as in stabilization loop (c), greatly improved the stability of the system.

Table I also indicates that when the roll-angle signal (azimuth stabilization loop (c) is replaced by a yaw-rate signal (loop (d)) the response becomes less stable. If the sideslip remains at zero during a turning maneuver the yaw rate r can be expressed as $(g \sin \varphi)/V$ or $g\varphi/V$ if the bank angle is not too large (see page 23). Thus, it appears that identical results should be obtained with either φ or r feedback, provided equivalent gains are used. The difference shown in table I is due primarily to the fact that it was not possible to operate the system with the yaw-rate feedback gain high enough to make the two networks equivalent ($|\delta A/r|$ should be 570 for equivalence with $|\delta A/\varphi| = 1.0$). Furthermore, any sideslip developed during the initial portion of the maneuver would influence r to a greater extent than φ. The high gain levels required in azimuth stabilization loop (d) produced unstable tendencies which were undesirable for these preliminary flight tests.

The turn coordination channel, which controls the rudder to maintain sideslip angles near zero, was developed on the simulator concurrently with the azimuth channel tests. Pulse disturbances, corresponding to v_a in figure 5(b), were introduced into the azimuth channel and the various rudder parameter gains were adjusted to give optimum coordination. As shown in figure 5(b), signals proportional to yawing velocity, sideslip angle, and rolling velocity were fed to the rudder to attain the desired turn coordination. Subsequent flight tests indicated better turn coordination under automatic control than was realized under manual control in similar maneuvers. This turn coordination network was used in all flight tests under automatic control, although flight results indicated that the test vehicle was not particularly sensitive to certain circuit parameter changes (for example, the rolling-velocity feedback signal could be omitted without serious deleterious effects).

Preliminary tracking studies.- Preliminary flight tracking studies against nonmaneuvering and maneuvering targets were conducted with the simple error-signal command system and with the stabilization networks just discussed. Tracking runs, at a pressure altitude of 10,000 feet and at an airspeed of 180 knots, were made against nonmaneuvering targets starting from a tail chase with a 100-mil initial step "lock-on" error below or to the right of the target in elevation and azimuth, respectively.

These flight tracking studies indicated that the best tracking in elevation would be realized with a loop incorporating elevation stabilization loop (c) (pitching-velocity feedback). The best azimuth-tracking for these preliminary studies was obtained with the azimuth-stabilization loop (c) (roll angle and rolling-velocity feedback). Time histories of these tracking results are shown in figure 6 compared with similar tracking results obtained under manual control by an experienced pilot[1] (the small random errors in both modes of control have been faired for clarity). This comparison offers a convenient basis for critically assessing the automatic tracking performance with the simplified system and for highlighting deficiencies requiring further study and system improvements. In all cases, the time required to reduce and maintain the initial tracking error within ±5 mils was greater under automatic control. This is particularly noticeable in azimuth error where the time to reduce the error is in excess of 32 seconds.

It was noted that azimuth tracking with tight roll stabilization, loop (c), was not as good as when the moderately stabilized loop (d) was used, primarily because tight roll stabilization restricted the bank-to-turn airplane in roll and hence reduced its ability to correct azimuth errors rapidly. However, azimuth stabilization loop (d) was not selected for further study at this time because of undesirable stability characteristics as previously mentioned.

The tracking performance of the automatically controlled airplane with the simple command system was also investigated against a maneuvering target where the target executed a sudden breakaway turn. The best results were obtained with elevation stabilization loop (c) and with the azimuth stabilization loop (c) shown in table I. In a steady 2 g target maneuver, large steady-state errors, of the order of 120 mils in azimuth and 40 mils in elevation, built up within 6 seconds after the maneuver was initiated. These errors were off scale on the data cameras and hence a time history of this maneuver cannot be presented. In these maneuvers, the automatically controlled airplane was well stabilized and the tracking was smooth; however, it was evident that system modifications would be required to eliminate this type of error in steady turns.

Automatic Control With an Improved Command System

The preliminary flight tests of the automatic control system with a simple command loop showed that the tracking performance was seriously limited by the inability to reduce azimuth errors rapidly and by the inability to track steady maneuvering targets without steady-state errors.

[1] The manual-control data presented in this report were obtained by Mr. Rudolph D. Van Dyke, Jr., pilot A of reference 9.

[redacted]

It appeared that these limitations could be corrected by the addition of suitable networks between the command circuit and the stabilization loop (for convenience, such signal-modifying networks will be considered hereafter as part of the command circuit). Improvements of this type could best be developed on a simulator; a Reeves Electronic Analog Computer with sufficient capacity to permit an adequate simulation of the desired maneuvers was available for this purpose.

Initial REAC simulation.- The details of the REAC investigation and the development of the associated equations are given in Appendix A, key points of which are included in the following discussion. A block diagram of the system simulated on the REAC is shown in figure 7. For the purpose of this simulation, it was necessary to make the following assumptions:

1. perfect turn coordination ($\beta = 0$)
2. perfect tracking ($\epsilon = \lambda$)
3. second-order rate-limited servo system
4. second-order airplane response in pitch
5. first-order airplane response in roll (negligible roll-yaw coupling and negligible roll due to rudder)

It was also necessary to give careful consideration to the simulation of the problem kinematic parameters such as range, relative velocities, inclination of the interceptor gun line, and the rotation and translation of the interceptor with respect to the target during maneuvers. The effects of range and the favorable effect, on the tracking performance, of a 5° inclination of the interceptor gun line are discussed in some detail in Appendix A.

In order to insure a valid starting point for the REAC synthesis of circuit improvements, the optimum simplified automatic control system (elevation stabilization loop (c), azimuth loop (c), and simple command circuit) was simulated and REAC results were compared with the corresponding flight results to establish the validity of the stabilization-loop simulation (fig. 8) and the tracking-loop simulation (fig. 9). The small discrepancies are within the repeatability of flight runs with the same parameter adjustments and are due primarily to small nonuniformities in the operation of the radar simulator and minor differences in range, airspeed, etc., between flight and the REAC.

Development of the nonlinear command network.- Following the establishment of a valid simulation of the system containing the simple command circuit, attention was turned toward utilizing the REAC for studying means of overcoming the major deficiencies demonstrated in the initial flight tests. First, consideration was given to means of minimizing the time (see fig. 9) for the automatically controlled interceptor to reduce initial 100-mil azimuth tracking errors to a reasonably low value (say ± 5 mils). The data in figure 9 represent the best compromise azimuth tracking performance with a linear command-signal gain. Increasing this linear gain was found to give superior tracking for small errors at the expense

of excessively large overshoots in the initial maneuver (due to rate-limiting of the aileron servo system), with a net increase in the time required to reduce the original error. Likewise, lowering the linear gain reduced the initial overshoots but provided inadequate control for small errors. Hence, it appeared that some form of nonlinear gain in the azimuth command circuit (high gain for small errors, low gain for large errors) could be used to advantage to permit a more rapid reduction of both large and small azimuth errors.

Several types of nonlinearities were studied on the REAC. The most promising nonlinearity is shown in figure 10. A significant improvement in tracking performance was predicted on the REAC when this nonlinear command network was used (fig. 11). The corresponding aileron control motions are also shown in figure 11. The large early reversal of the aileron angles, needed to prevent large initial overshoot, results from the use of high gains for azimuth tracking errors less than $1/2^{\circ}$ (8.7 mils).

A nonlinear gain device which approximated the characteristics selected from the REAC study was installed in the airplane and successfully flight tested. The nonlinearity predicted on the REAC was modified as shown in figure 10 to prevent severe twitching of the ailerons at the break point. Quantitative comparison of REAC and flight tracking performance with this and other system improvements will be discussed later. Additional examples of the use of the nonlinearities are given in reference 10.

Development of integrating networks for eliminating steady-state errors.- The preliminary flight tests with the simple command circuit also indicated that large steady-state errors would occur when the interceptor attempted to track a target in a steady turn. The diagram below

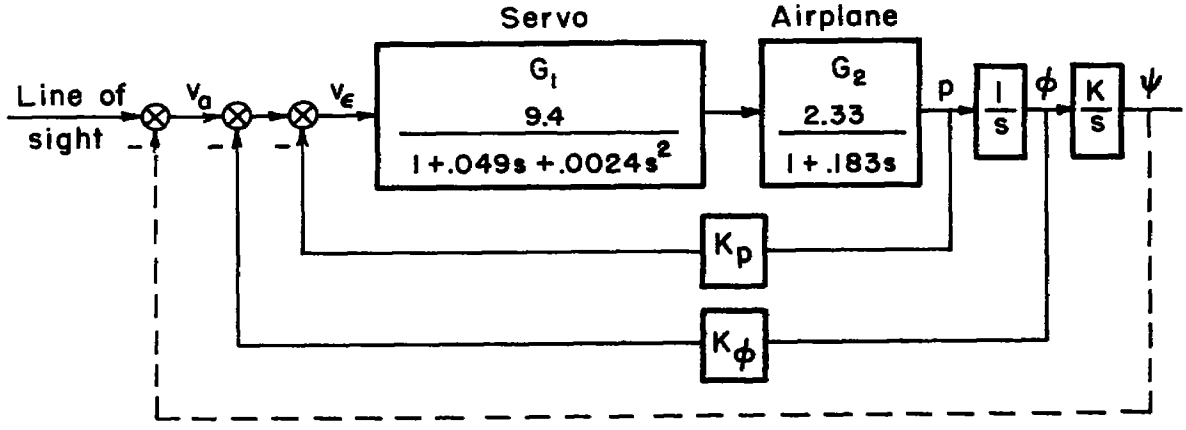

$$\frac{\psi}{V_a} = \frac{KG_1G_2}{s\left[(1 + K_pG_1G_2)s + K_\phi G_1G_2\right]}$$

Sketch (b)

[redacted]

represents the azimuth channel of this system, with the assumption that for small bank angles, $\dot{\psi} = K\varphi$ where $K = g/V$. This system, with its $1/s$ term in the open-loop transfer function, will produce a steady-state error when subjected to a constant velocity input since a finite value of the error voltage v_a must exist if the bank angle φ required for the turn is to be maintained (see, e.g., p. 208 of ref. 11). The addition of a properly designed integrating network (essentially integrating the azimuth error signal) as shown in the diagram below changes the transfer function as follows:

$$\frac{\psi}{v_a} = \frac{KG_1G_2(K_V + s)}{s^2[(1 + K_pG_1G_2)s + K_\varphi G_1G_2]}$$

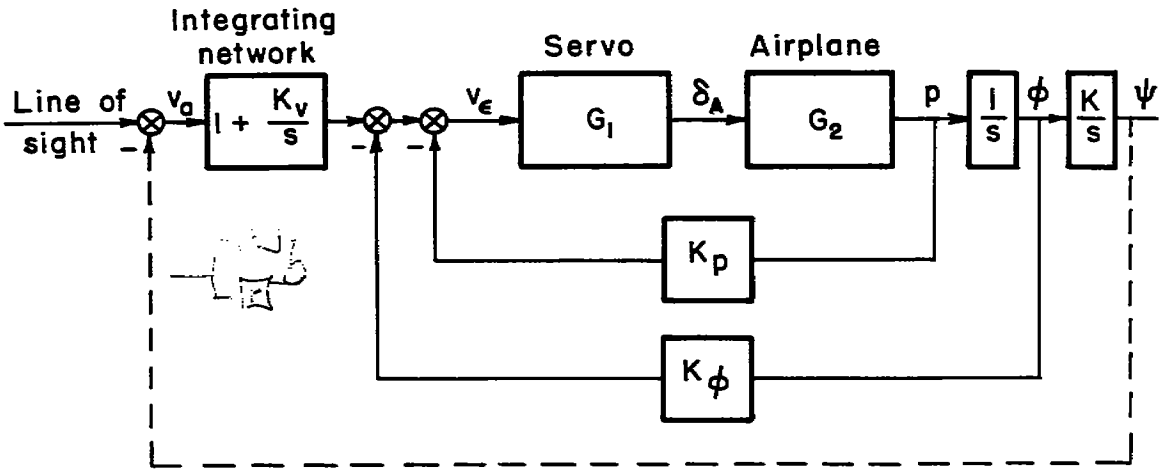

Sketch (c)

This open-loop transfer function has a $1/s^2$ characteristic term and does not require a constant error voltage v_a to maintain the bank angle φ in the steady turn maneuver. A short-term transition error will exist when the maneuver is initiated but will be reduced at a rate dependent upon the gains in the system. A similar analysis can be applied to the elevation channel.

REAC studies were conducted to determine the optimum gains, K_{V_e} and K_{V_a} (fig. 7), of the integrating networks. The improvement in the predicted tracking performance in response to an 8° per second turning command associated with the addition of the integrating networks is illustrated in figure 12.

The integrating networks for both the azimuth and elevation channels were mechanized by means of electronic circuits, installed in the test airplane, and were successfully flight tested at the gain levels indicated by the REAC studies. Comparison of the predicted and measured effects of

the integrating networks on the transient tracking performance is included in the next section.

Preliminary tracking studies with the improved command system.— Automatically controlled tracking runs in maneuvers similar to those previously used with the simple command system were conducted in flight and were simulated on the REAC using the improved automatic control system which consisted of the azimuth and elevation stabilization loops (c) of table I modified by both the nonlinear and integrating networks in azimuth and an integrating network in elevation as just described.

The tracking performance, with this improved automatic control system, during a lock-on maneuver against a nonmaneuvering target is shown in figure 13. Although the integrating network reduced the predicted large favorable effect (shown in fig. 11) of the nonlinear gain on the transient azimuth tracking performance, it is readily seen that the combined modifications still gave a marked improvement over the simple-command-system performance shown in figure 9. The time to reduce the azimuth error to within ±5 mils has been reduced from a time in excess of 32 seconds (fig. 9) to approximately 7 seconds (fig. 13). No material change in performance was experienced in the elevation channel. Again, the correlation between the flight and REAC data is considered excellent.

Next, the tracking performance of this improved automatic control system against maneuvering targets was checked in flight. No quantitative comparison can be made between these flight-test results and the REAC studies shown in figure 12 because the step turning command input used on the REAC does not simulate the initial transient conditions which occur when the target airplane initiates the turn. However, the time history of a typical flight run (fig. 14) shows that, as might be predicted from figure 12, the integrating networks successfully eliminated the steady-state errors in the steady turn (about 2 g in this example) but that a large azimuth error occurred in the turn-entry transition region.

The lengthy interval of large azimuth transition error might be ascribed, in part, to the tight roll-stabiliazation characteristics of the roll-angle and roll-rate stabilization loop and in part to the lack of target bank-angle signals, which are used by a human pilot to anticipate target evasive turns. This latter difficulty is inherent in known target seekers, and it was apparent that any system improvements must come from changes in the azimuth roll-stabilization loop. Preliminary flight studies indicated that azimuth stabilization loop (d) (table I) permitted a more rapid reduction of a large initial azimuth error than stabilization loop (c). However, as previously indicated, loop (d) was initially considered less desirable from the over-all flight standpoint because of unstable tendencies due to low damping characteristics and the high gain levels required.

In an effort to improve the transition-region tracking performance, azimuth stabilization loop (c) was replaced with stabilization loop (d). A comparison of the flight azimuth tracking performance in the transition region is shown in figure 15 for both stabilization loops (c) and (d) and for a typical manually controlled maneuver. It is seen that, compared to loop (c), the more loosely stabilized loop (d) reduced several-fold the errors in the period immediately following initiation of the target evasive turn; although still somewhat larger than when under manual control, the errors with loop (d) were at least of the same order of magnitude. The over-all tracking performance as measured in the lock-on maneuver with a 100-mil initial error, in steady straight flight and in steady turning flight, was not materially affected by the use of azimuth stabilization loop (d).

In view of the above results, azimuth stabilization loop (d) of table I was used in all succeeding analytical and flight studies. The associated complete automatic control system, representing the optimum compromise for the various tracking problems considered, is summarized in block-diagram form in figure 16. Pertinent transfer functions for the servos and airframe, for the azimuth nonlinear gain, for the integrating networks, and for the feedback gains have been given in figures 5, 10, and 12, and table I, respectively.

Effects of combined azimuth and elevation errors at lock-on.- Prior to proceeding with a more complete evaluation of the automatic control system shown in figure 16, it was desirable to examine briefly the effects of combined azimuth and elevation errors at the time of lock-on, since, as indicated in the diagrams below, there are target-interceptor situations which may cause tracking instabilities in the attacking airplane.

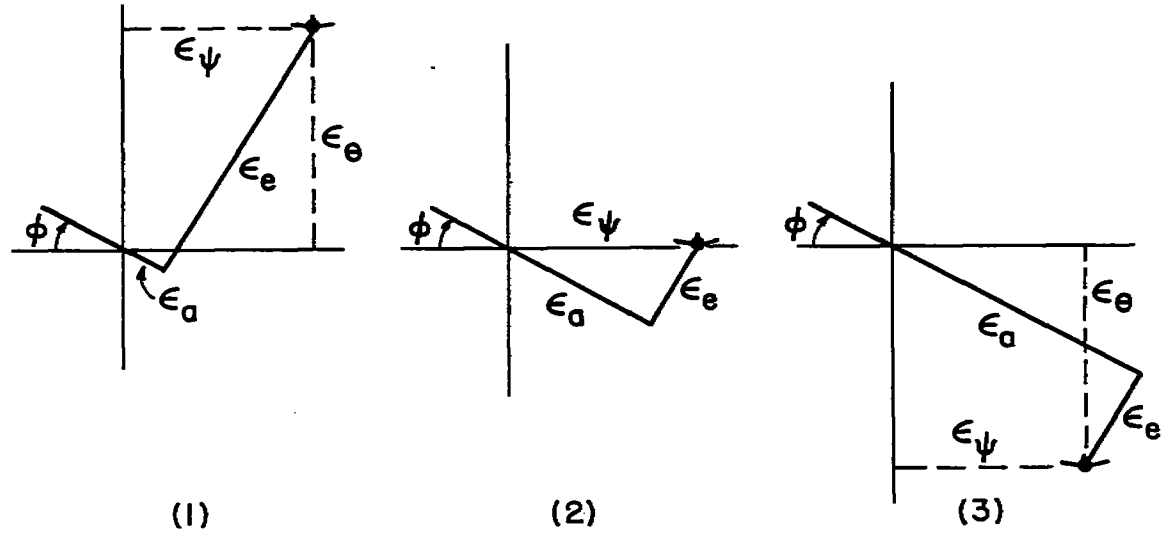

Sketch (d)

These diagrams show three tracking situations where the target has the same azimuth error ϵ_ψ but different elevation errors ϵ_θ. When the target is above the interceptor as in diagram (1), or when there is no elevation error as in diagram (2), banking the interceptor toward the target tends to reduce the error ϵ_a. However, when the target is below the interceptor, as in diagram (3), it is apparent that the banking of the interceptor to correct the azimuth error ϵ_a initially increases this error. This destabilizing effect becomes acute as the target approaches a position directly under the interceptor gun line.

These effects were initially studied on the REAC and the results are shown in figure 17. These data represent the path of a projection of the interceptor gun line on a plane through the target, perpendicular to the initial interceptor gun line. These REAC data indicate that this interceptor will not experience the unstable conditions shown above in diagram (3) because, as shown in figure 17(c), the interceptor pitched so rapidly at lock-on that the relative position of the target was changed from below the interceptor to above the interceptor where the instabilities did not exist. For example, at approximately 0.7 second after lock-on (fig. 17(c)) the initial pitch error had been wiped out and yet the bank angle had only reached the relatively low value of 10°, which was too small to cause any sizable unstable tendency. Also, as shown in figure 17(a), the interceptor overshot the target by approximately 100 mils in less than 2 seconds so that its position, relative to the target, was similar to that shown in figure 17(c). In this case, however, the bank angle was about 40° (at $t = 2$ seconds) and the apparent elevation error ϵ_e was almost zero; thus the tendency toward instability had no effect. The high ratio of pitch response to roll response is reflected also in the data shown previously in figures 6, 9, and 13.

Similar flight maneuvers confirmed these REAC results. However, these maneuvers exceeded the photographic range of the tracking cameras and hence flight time histories of these maneuvers are not available.

Evaluation of the Automatic Control System in Typical Final Attack Maneuvers

Previous sections of this report have been devoted to flight and analytical studies of various stabilization loops and command networks for use in an automatically controlled interceptor. From these studies of segments of the total interceptor guidance problem, a more or less optimum automatic control system was developed (fig. 16) which produced the best tracking performance for all of the attack situations considered. It is of interest to evaluate further the tracking performance of this selected automatic control system in a more comprehensive series of flight tests which impose a wider variety of interceptor motions representative of those that might be encountered with a tactical interceptor, and to

compare quantitatively and statistically the tracking performance of the automatically controlled interceptor (and the radar simulator) with the tracking performance of the manually piloted airplane.

The flight-test maneuvers used in this evaluation were the Ames standard gunnery run (ASG runs), shown in figure 18(a) and described in detail in reference 9, and a 90° beam attack shown in figure 18(b). These maneuvers provided target-interceptor motions comparable to most phases of an automatic attack requiring precise roll, pitch, and yaw control. The ASG run may be recognized as a composite of the test maneuvers used in the preliminary studies.

Comparison of the airplane tracking performance under automatic and manual control.- Typical time histories of the gun-line wander during automatically controlled ASG runs and 90° beam attacks are compared in figures 19 and 20, respectively, with similar time histories obtained under normal manual control. It is seen that in all cases the tracking was smoother and more precise under automatic control, except during the brief lock-on and transition periods.

The gun-line wander in a series of 90° beam attacks and in the straight-flight and steady-turn portions of a number of ASG runs was analyzed statistically. In all cases, bias errors were very small for both automatic and manual control. Analysis of over 20,000 data points showed that the tracking error distribution was approximately Gaussian. The average standard deviations of the gun-line wander during the selected portions of the test maneuvers are shown in the following table.

Average standard deviation of the gun-line tracking error, σ, mils		
Target maneuver	Automatic	Manual
Azimuth		
Nonmaneuvering	1.1	2.1
Maneuvering		
Standard gunnery run	1.5	2.9
[a]90° beam attack	1.5	2.7
Elevation		
Nonmaneuvering	1.1	2.2
Maneuvering		
Standard gunnery run	2.9	3.2
[a]90° beam attack	2.9	3.1

[a]Does not include initial transient.

It is seen in the table above that although the standard deviations of the tracking errors under manual control were small, in all cases they were even smaller under automatic control. The practical importance of such numerically small improvements in tracking accuracy due to

automatic control would depend on such factors as the particular armament, tactical situation, and fire-control system under consideration.

The initial portions of the test maneuvers and the transition region of the ASG runs are of a transient nature that did not appear amenable to any useful statistical analysis. Information regarding the length of the transient region and the magnitude and nature of the tracking errors is, of course, contained in the tracking-error time histories shown in figures 19 and 20. Although the transient errors under automatic control were in general larger than under manual control, the differences were not considered excessive in view of the unavoidable loss of useful target bank-angle information mentioned previously.

Evaluation of the optical tracking performance with the radar simulator.- A statistical evaluation of the tracking performance of the optical radar simulator during the test maneuvers is of interest because this device has a marked influence on the over-all tracking performance of the automatically controlled airplane. Typical time histories of the optical tracking with the manually operated radar simulator during test maneuvers with the automatic control system shown in figure 16 are given in figure 21. The small step-like discontinuities shown on these time histories are primarily the result of aileron twitching (at the break points of the azimuth nonlinear gain), target wake effects (in the transition region and in turning flight), and the characteristic stepwise motions of the sight operated in elevation (due to high breakout forces).

The average standard deviation of the line-of-sight error (radial) for all of the test maneuvers was less than 1 mil.[2] For comparison, the average standard deviation of the radial gun-line error when under manual control was approximately three mils against nonmaneuvering targets. The high quality of the tracking performance with the optical radar simulator is associated with the superior dynamic response characteristics of the small mechanical device as compared with that of the airplane and its control system. Thus, the optical sighting station approximated the action of a noise-free, lag-free radar, so that (as desired for the present study) airplane tracking errors arising from erroneous target information were very small. Even with much less stable airplane-autopilot conditions, such as azimuth stabilization loop (a) in table I, the tracking performance of the line of sight was very good.

The excellent tracking performance attained with this manually operated optical device suggests that tracking equipment, based on this principle, might prove useful in the design of director-type fire control systems.

---

[2]The operation of the optical radar simulator in flight, the precise control of which contributed so much to the success of this project, was accomplished by Mr. Donovan R. Heinle, pilot C of reference 9.

CONCLUSIONS

Flight and analog computer studies of the final-attack phase of an automatically controlled interception are described in this report. The flight tests were made in a low-speed propeller-driven airplane with a simulated noise-free radar. Pure pursuit tracking runs with a number of initial attack situations were used as a basis for testing various types of airplane stabilization and command loops. Due to numerous differences in attack problems, airplane and component performance, and system complexity between this test equipment and present and projected automatic interceptors, the following conclusions based on the methods and results of the present study alone cannot be applied indiscriminately to the synthesis of high performance systems; the extent to which they are applicable will depend on the individual situation.

1. Of the various control systems investigated, the one giving the most favorable tracking characteristics for the different test maneuvers incorporated pitch-rate stabilization in the elevation channel and roll rate and yaw rate in the azimuth channel.

2. The use of integrating networks in both channels was found to be a satisfactory means for eliminating the steady-state errors normally associated with the tracking of a steadily maneuvering target without necessitating the use of increased system gain levels, a point of general interest in system design.

3. Poor yaw response associated with aileron servo rate limiting was significantly improved through the use of a nonlinear gain in the azimuth channel. A device of this type provides a fast and stable response with a relatively low-powered rate-limited servo and hence may have many possible applications.

4. An automatic rudder turn-coordination system, designed on the basis of analog-computer studies was used successfully in all flight tests to maintain sideslip angles near zero.

5. The adequacy of the simulation procedures employed in the analog-computer studies of this investigation was verified by the subsequent flight tests.

6. Analog-computer studies showed a strong favorable effect on airplane tracking performance of the 5° gun-line inclination employed in the test airplane to avoid the wake of the target.

7. With the selected automatic control system, tracking of airborne targets was generally smoother and more precise than manually controlled tracking. For example, in steady straight tail-chase runs, the standard deviations of the gun-line wander in azimuth and elevation under automatic control were about one mil and under manual control about two mils.

Although somewhat larger errors were experienced in transient conditions under automatic control than under manual control, they were not considered excessive. Bias errors were always very small under either mode of control.

8. The average radial standard deviation of the tracking-line wander of the manually operated optical sighting device used to simulate a noise-free radar was less than 1 mil. This excellent tracking performance with the movable optical sighting device may be of interest in connection with the design of director-type fire-control systems.

Ames Aeronautical Laboratory
National Advisory Committee for Aeronautics
Moffett Field, Calif., Oct. 14, 1954

APPENDIX A

SIMULATION OF AUTOMATIC INTERCEPTOR PROBLEM ON THE ANALOG COMPUTER

The Reeves Electronic Analog Computer was used to simulate the automatically controlled interceptor described in this report. This simulation included the geometric loops involved in tracking of a non-maneuvering target with initial lock-on errors in azimuth and elevation. The block diagram of the complete network shown in figure 7 is based on the following assumptions:

1. There is a perfect rudder channel maintaining zero sideslip at all times.

2. The roll-angle response of the airplane is defined by the transfer function

$$\frac{\varphi}{\delta_A} = \frac{12.7}{s(s + 5.46)}$$

This single-degree-of-freedom representation neglects roll due to yaw, and for the condition of zero sideslip the yawing velocity may be expressed as $r = (g/V) \sin \varphi$.

3. The airplane pitching-velocity response may be represented by the second-order transfer function

$$\frac{q}{\delta_E} = \frac{-19.5(1 + 0.75s)}{s^2 + 3.72s + 1.8}$$

which is of the form ordinarily obtained when changes in forward speed are neglected.

4. The elevator and aileron servos can be represented as second-order systems with control rate limiting.

5. The human sight operator tracks the target perfectly, that is, has a unity transfer function ($\epsilon = \lambda$).

6. The distance between target and interceptor remains constant during a tracking run.

In figure 7, the initial lock-on errors ϵ_{ψ_o} and ϵ_{θ_o} (with respect to horizontal and vertical space axes) are programmed at the left as step inputs. The error signals ϵ_ψ and ϵ_θ must then be resolved into the airplane coordinate system to produce the tracking errors ϵ_e and ϵ_a. In general, when the reference axis of the sight is coincident with the

roll axis of the airplane and when the angular displacements are small, the resolution can be accomplished as shown in the sketch below:

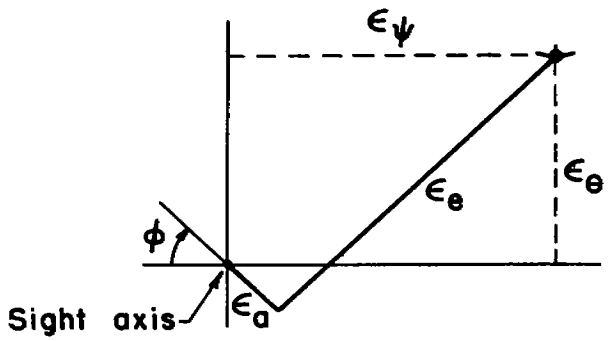

Sketch (e)

where

$$\epsilon_e = \epsilon_\theta \cos \varphi + \epsilon_\psi \sin \varphi$$

$$\epsilon_a = \epsilon_\psi \cos \varphi - \epsilon_\theta \sin \varphi$$

In the SB2C-5 airplane, however, the sight axis was inclined upward from the roll axis by an angle η of approximately 5°. The following sketch illustrates the correct resolution in this case:

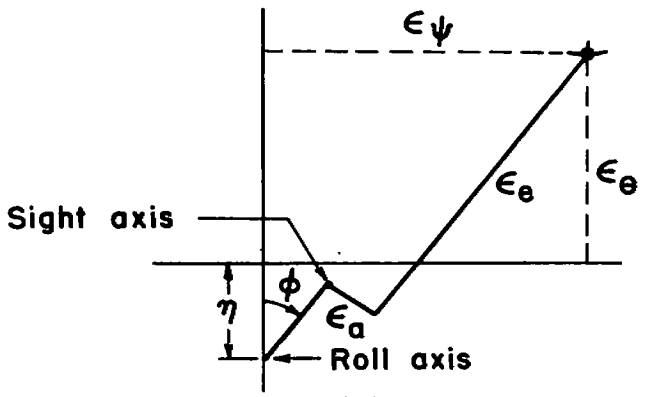

Sketch (f)

Here ϵ_e and ϵ_a may be expressed as

$$\epsilon_e = \epsilon_\psi \sin \varphi + (\epsilon_\theta + \eta) \cos \varphi - \eta$$

$$\epsilon_a = \epsilon_\psi \cos \varphi - (\epsilon_\theta + \eta) \sin \varphi$$

This is the resolution shown in figure 7 (Resolver No. 1).

[redacted]

By comparing the two preceding sketches, it can be seen that with a positive angle η there is a reduction in ϵ_a as the airplane rolls. This means that smaller bank angles are required to eliminate a given azimuth error; thus, as indicated in reference 12, the offset gun line appears to be a stabilizing influence. This contention was verified with the analog computer where tracking runs with 100-mil initial azimuth errors were simulated with various values of gun-line inclination, η. Figure 22 shows the results for $\eta = 0^\circ$ and $\eta = 5^\circ$. At $\eta = 0^\circ$, the response is only marginally stable. This response could be made satisfactory only by reducing the gain for the optical radar simulator. As shown in figure 22, the tracking with the gun axis inclined 5° nose up (with respect to the fuselage datum line) was much superior to tracking with the gun line parallel to the fuselage datum line.

Returning to figure 7, the resolved error signals ϵ_e and ϵ_a are then modified by the sight gains K_{λ_e} and K_{λ_a}, are further modified by the integrating networks, and then are fed to the proper servos. It can be seen that the inner stabilizing loops are the same as used in the airplane except that the rudder channel has been omitted. With the assumption of zero sideslip and small pitch angles, the airplane turning rate r can be expressed as a simple function of the bank angle Φ as shown in the following acceleration diagram:

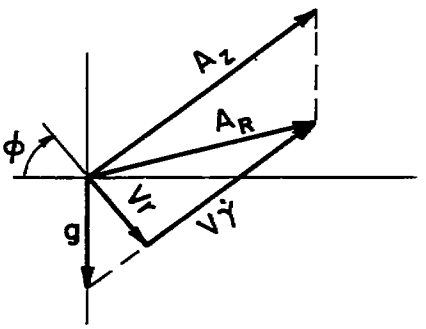

Sketch (g)

The accelerations A_Z and g are added vectorially to give the resultant A_R which may be resolved into the components Vr and $V\dot{\gamma}$, normal and parallel, respectively, to A_Z. From the sketch it can be seen that $Vr = g \sin \Phi$. This expression eliminates the necessity of knowing the airplane yaw responses for aileron and rudder deflections.

The airplane responses q and r must then be resolved to obtain the rates $\dot{\theta}$ and $\dot{\psi}$ with respect to space axes. Since $q = \dot{\gamma} + \dot{\alpha}$ the proper resolution (Resolver No. 2) is illustrated in the following sketch.

[redacted]

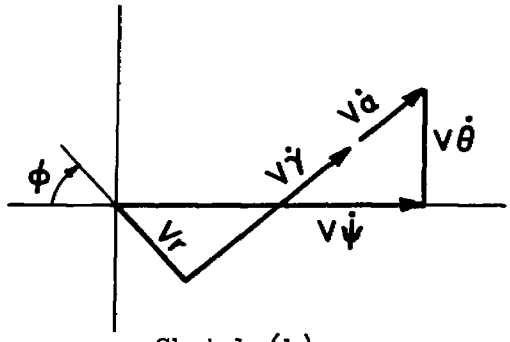

Sketch (h)

$\dot{\theta} = q \cos \varphi - r \sin \varphi$

$\dot{\psi} = q \sin \varphi + r \cos \varphi$ (when, as in the present case, θ is always small)

These quantities are then integrated to give the angles turned through by the attacker.

To complete the geometric representation of the tracking maneuver, the translation of the attacker normal to the flight path must also be considered. The following sketch illustrates the lateral translation; a similar case exists in pitch.

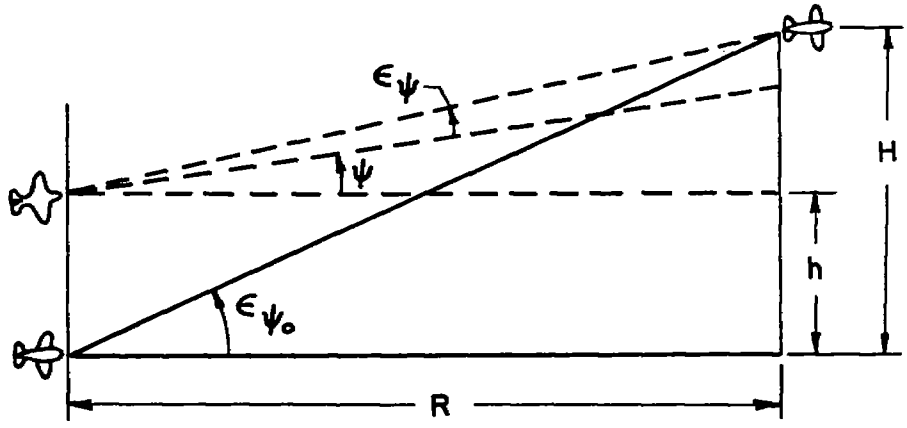

Sketch (i)

After time t the attacker has turned through an angle ψ and moved laterally a distance h, so that the tracking error has been reduced from ϵ_{ψ_o} to ϵ_ψ. With the assumption of small error angles and a constant range R, ϵ_ψ may be expressed as

$$\epsilon_\psi = \frac{H - h}{R} - \psi$$

[redacted]

or

$$\epsilon_{\psi} = \epsilon_{\psi_o} - \frac{h}{R} - \psi$$

The displacement h is approximately equal to $V \int_o^t \psi \, dt$. Thus

$$\epsilon_{\psi} = \epsilon_{\psi_o} - \psi - \frac{V}{R} \int_o^t \psi \, dt$$

The expression for h is based on the assumption that (in addition to $\beta=0$) $\dot{\alpha}$ remains small compared to q during the tracking maneuver, so that $\dot{\gamma}$ is approximately equal to q. In other words, the change in interceptor flight path is assumed to be the same as the change in attitude.

The range as it appears in the preceding equation has a marked influence on the performance of the interceptor while tracking after an initial lock-on error. In figure 23 are responses from the analog computer for a range of 600 feet and for an infinite range. This figure shows that as the range is reduced the problem becomes more severe and the response would tend to become unstable at very short ranges.

REFERENCES

1. Seamans, R. C., Jr., and Whitaker, H. P.: Dynamic Performance of Aircraft Tracking Systems. MIT Inst. Lab. Tracking Control Progress Rep. No. 6445-P-5, Sept. 1948.

2. Rea, James B.: Automatic Tracking of Aircraft. MIT Inst. Lab. Rep. 6445-T-8, 1947.

3. Recommendations for the Design of Automatic Interceptor Control Systems. MIT Inst. Lab. Rep. 6445-E-35.

4. Eckhardt, Homer D.: Design and Test of Rudder Components of an Airborne Tracking System. MIT Inst. Lab. Rep. 6445-T-14, 1948.

5. Oliver, T. K., and Healey, J. F.: Design and Test of the Aileron Components of an Airborne Tracking System. MIT Inst. Lab. Rep. 6445-T-12, 1948.

6. Turner, Howard L., White, John S., and Van Dyke, Rudolph D., Jr.: Flight Testing by Radio Remote Control - Flight Evaluation of a Beep-Control System. NACA RM A52A29, 1952.

7. Smaus, Louis H., Gore, Marvin R., and Waugh, Merle G.: A Comparison of Predicted and Experimentally Determined Longitudinal Dynamic Responses of a Stabilized Airplane. NACA TN 2578, 1951.

8. Turner, Howard L.: Measurement of the Moments of Inertia of an Airplane by a Simplified Method. NACA TN 2201, 1950.

9. Rathert, George A., Jr., Gadeberg, Burnett L., and Ziff, Howard L.: An Analysis of the Tracking Performance of Two Straight-Wing and Two Swept-Wing Fighter Airplanes With Fixed Sights in a Standardized Test Maneuver. NACA RM A53H12, 1953.

10. Schmidt, Stanley F., and Triplett, William C.: Use of Nonlinearities to Compensate for the Effects of a Rate-Limited Servo on the Response of an Automatically Controlled Aircraft, NACA TN 3387, 1954.

11. Chestnut, Harold, and Mayer, Robert W.: Servomechanisms and Regulating System Design. Vol. I. Wiley & Sons, Inc., 1951.

12. Pride, A. M.: Evaluation of Tracking Performance With Raised Sight Unit. (Letter Rep. 2, Tracking Accuracy Phase) Naval Air Test Center, Patuxent River, Md., Armament Test Div. TED PTR AR-6032, Serial AT-33-051, July 6, 1953.

[redacted]

TABLE I.- AIRPLANE RESPONSE CHARACTERISTICS WITH VARIOUS STABILIZATION LOOPS AS MEASURED IN FLIGHT AT 180 KNOTS, 10,000 FEET.

Elevation channel		Azimuth channel	
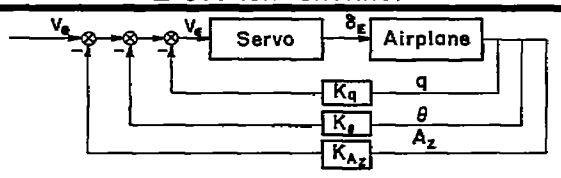		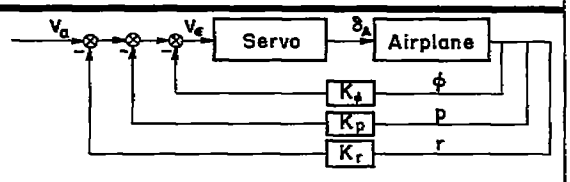	
Feedback gearing	Response to square pulse	Feedback gearing	Response to square pulse
$\frac{\delta_E}{\theta} = 1.5$ $\frac{\delta_E}{q} = 0$ $\frac{\delta_E}{A_z} = 0$ (a)	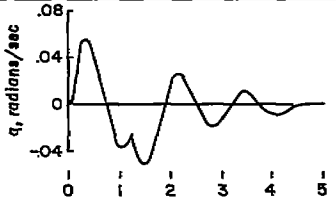	$\frac{\delta_A}{p} = -6.6 \frac{\text{deg}}{\text{radians/sec}}$ $\frac{\delta_A}{\phi} = 0$ $\frac{\delta_A}{r} = 0$ (a)	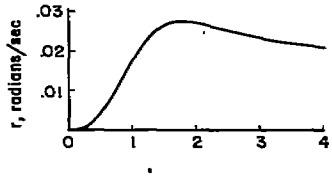
$\frac{\delta_E}{\theta} = 1.5$ $\frac{\delta_E}{q} = 46.8 \frac{\text{deg}}{\text{radians/sec}}$ $\frac{\delta_E}{A_z} = 0$ (b)	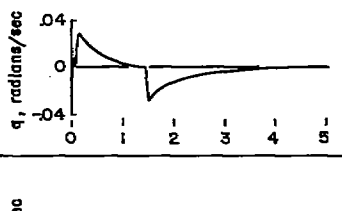	$\frac{\delta_A}{p} = 0 \frac{\text{deg}}{\text{radians/sec}}$ $\frac{\delta_A}{\phi} = -1.0$ $\frac{\delta_A}{r} = 0$ (b)	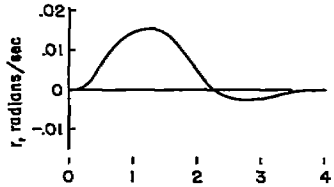
$\frac{\delta_E}{\theta} = 0$ $\frac{\delta_E}{q} = 46.8 \frac{\text{deg}}{\text{radians/sec}}$ $\frac{\delta_E}{A_z} = 0$ (c)	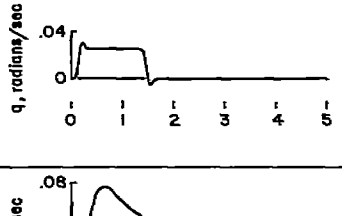	$\frac{\delta_A}{p} = -6.6 \frac{\text{deg}}{\text{radians/sec}}$ $\frac{\delta_A}{\phi} = -1.0$ $\frac{\delta_A}{r} = 0$ (c)	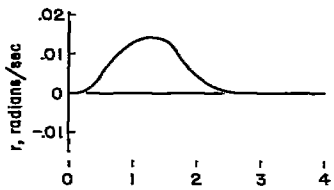
$\frac{\delta_E}{\theta} = 0$ $\frac{\delta_E}{q} = 0$ $\frac{\delta_E}{A_z} = 1.6 \frac{\text{deg}}{g}$ (d)	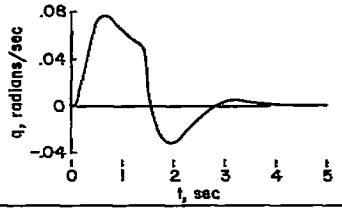	$\frac{\delta_A}{p} = -6.6 \frac{\text{deg}}{\text{radians/sec}}$ $\frac{\delta_A}{\phi} = 0$ $\frac{\delta_A}{r} = 323.0 \frac{\text{deg}}{\text{radians/sec}}$ (d)	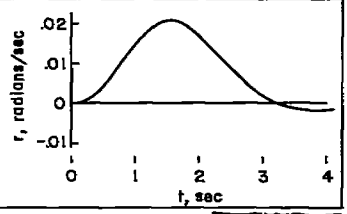

NACA

Figure 1.- Three-quarter view of test interceptor in flight.

A-17263

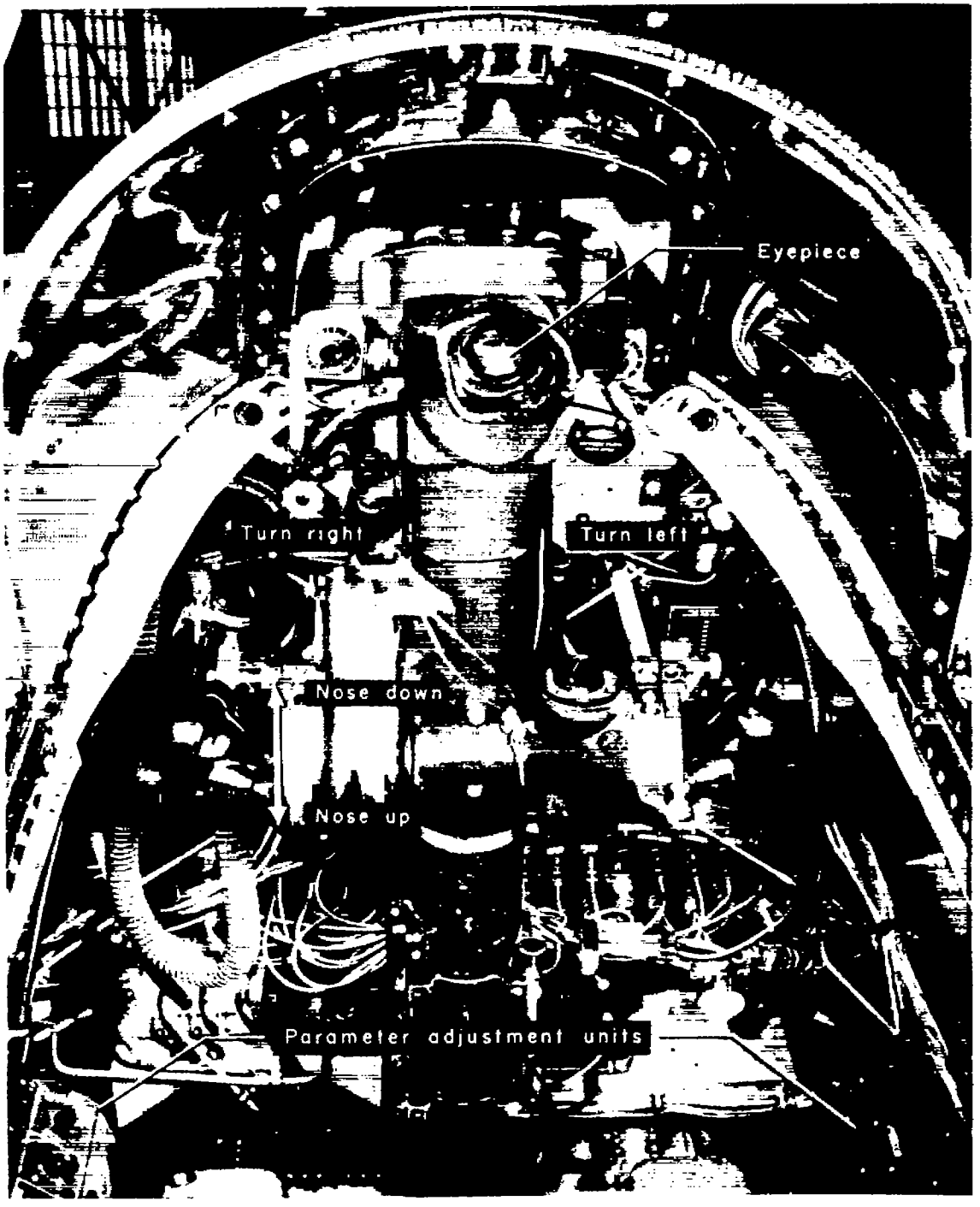

A-18847.1

Figure 2.— Optical radar simulator in rear cockpit of test interceptor.

[redacted]

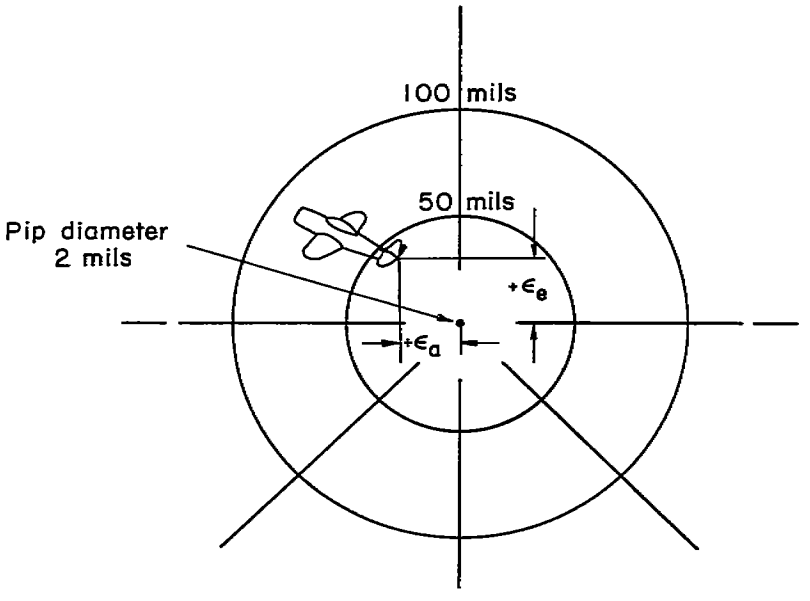

(a) Gun line.

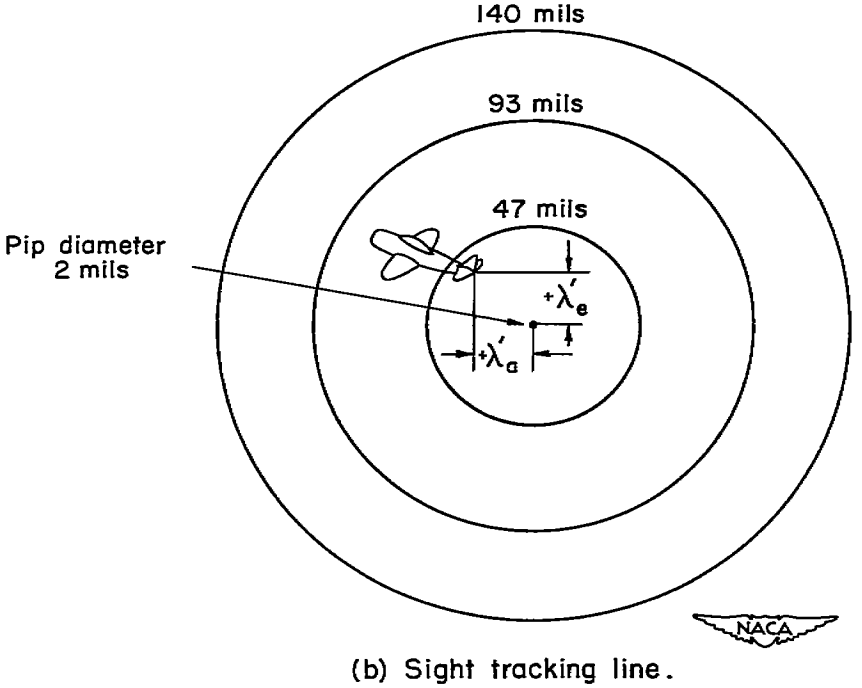

(b) Sight tracking line.

Figure 3.– Tracking errors as measured with 16–mm GSAP cameras.

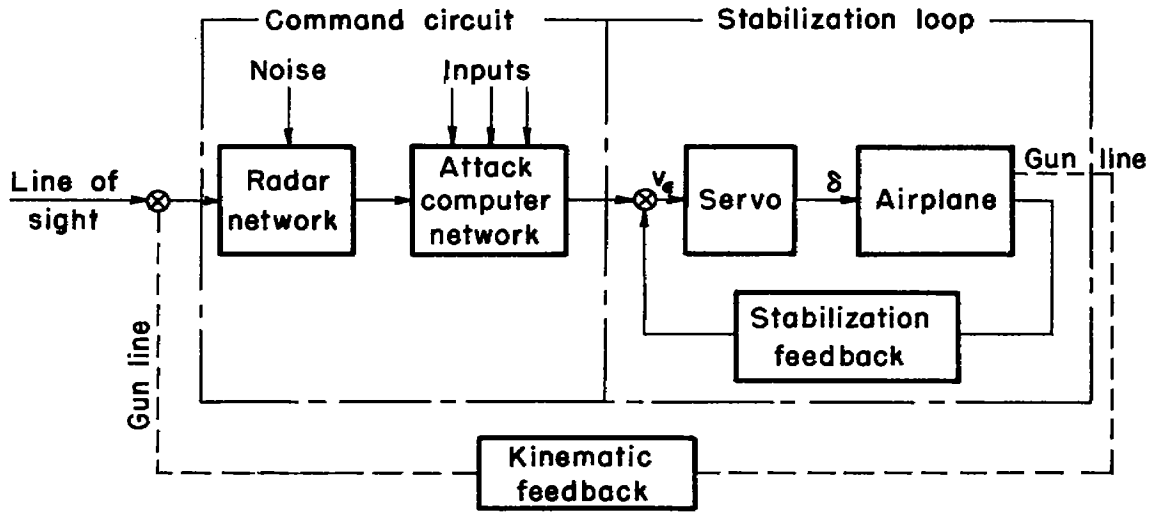

(a) Simplified representative automatic control system.

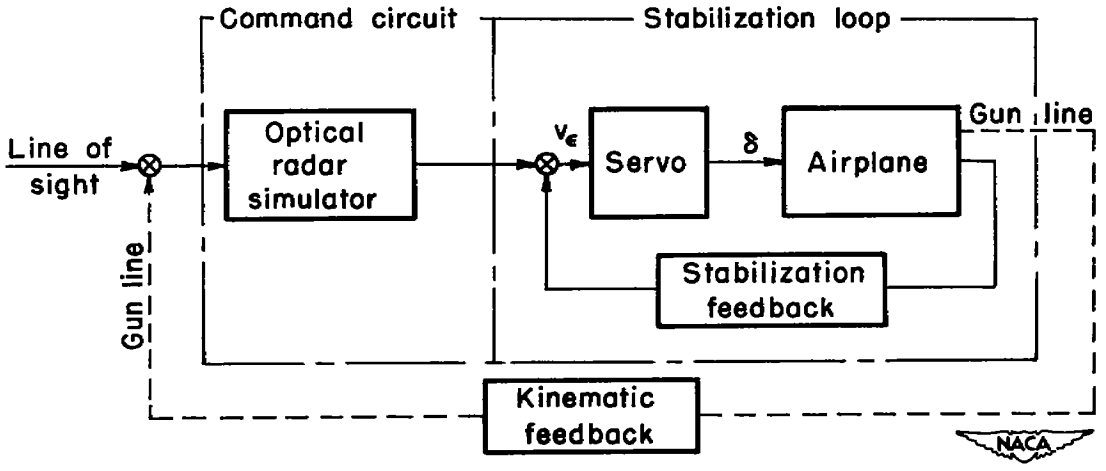

(b) Simplified SB2C-5 automatic control system.

Figure 4.— Block diagrams of simplified automatic interceptor control systems.

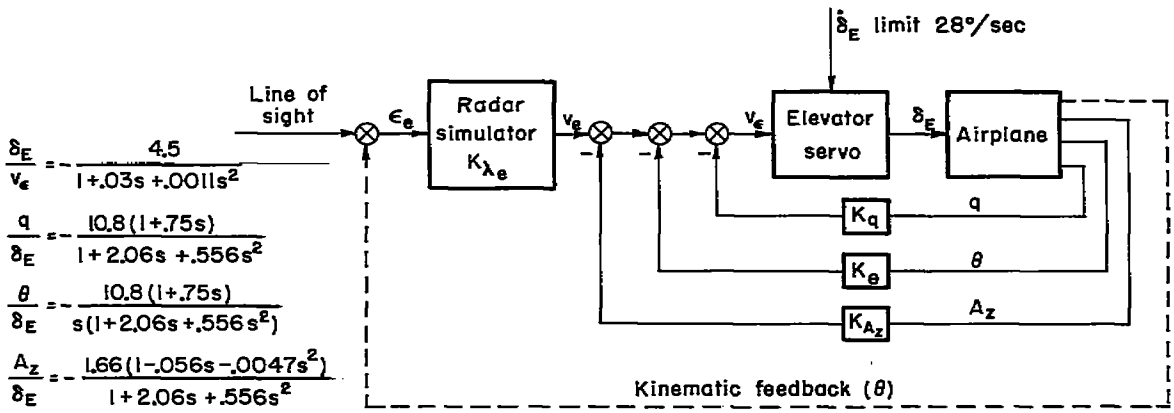

(a) Elevation channel.

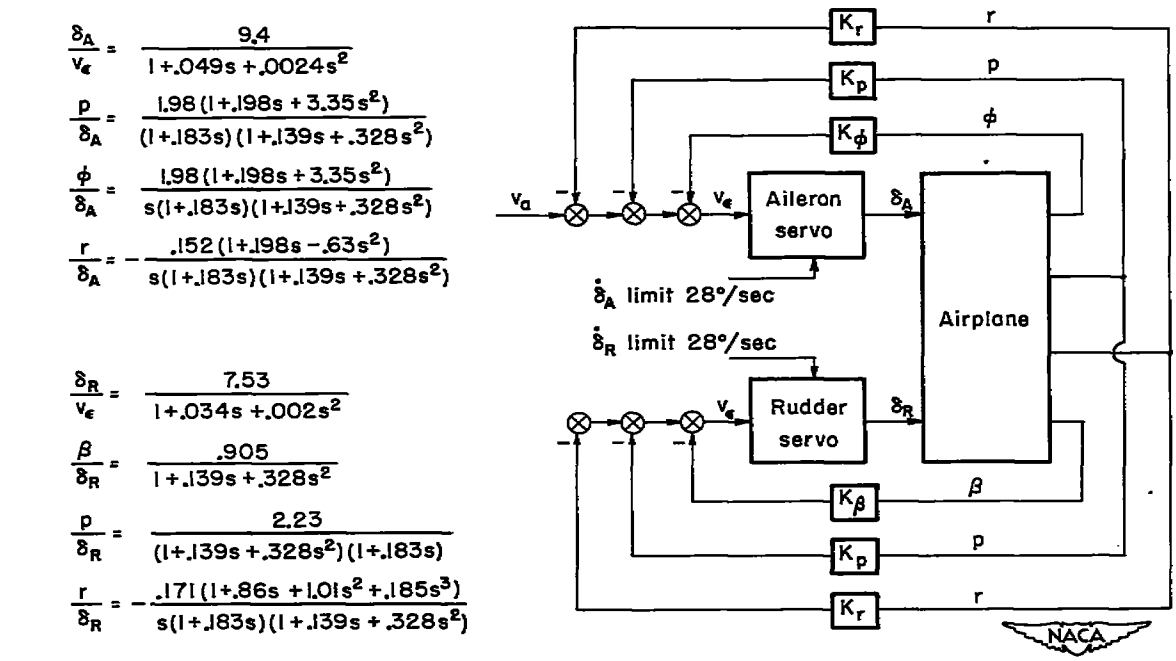

(b) Azimuth and turn coordination channels.

Figure 5.– Block diagram of automatic control system as studied on the high-speed electronic simulator.

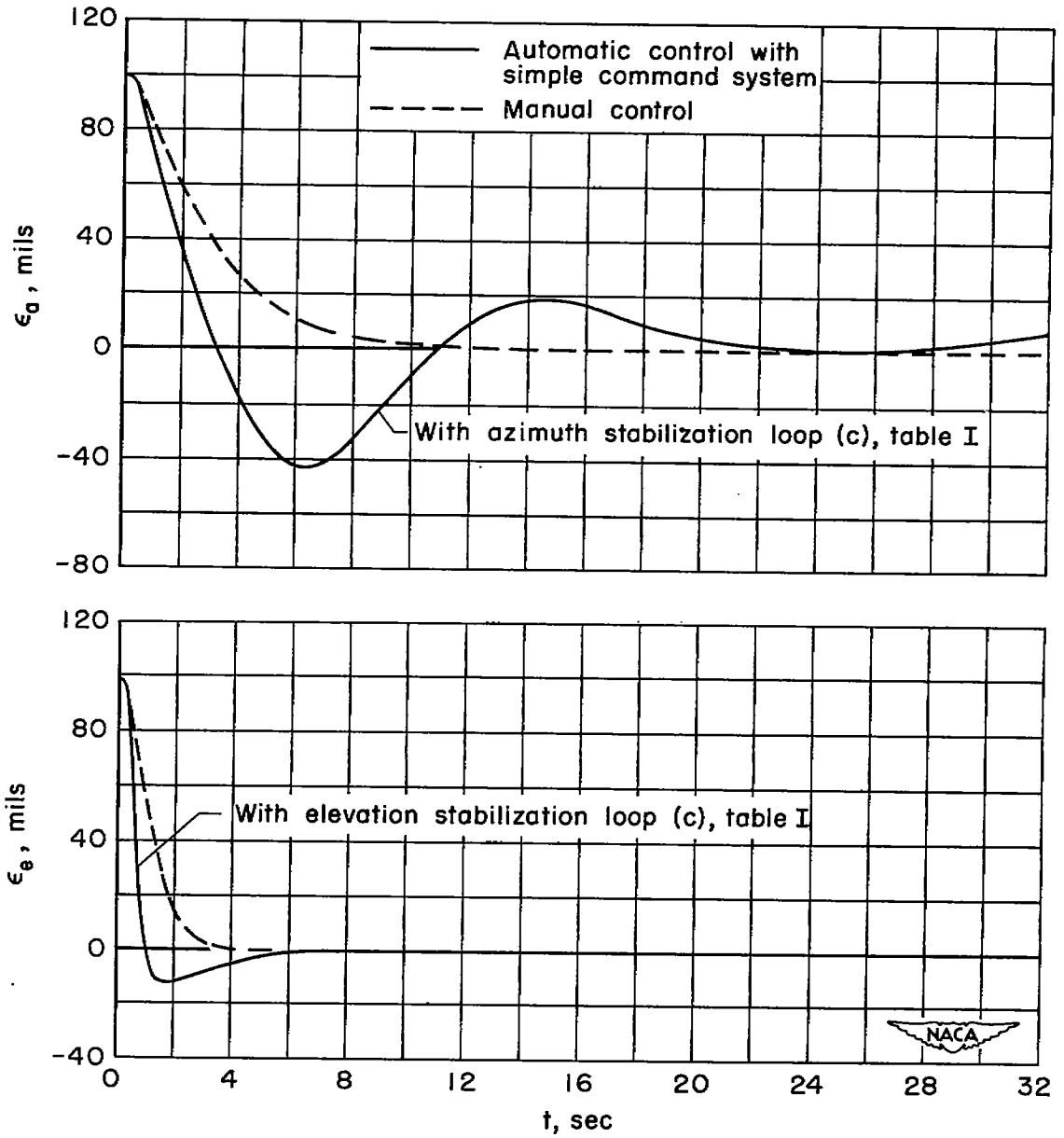

Figure 6.— Comparison of the tracking performance under automatic control and manual control during a lock-on maneuver.

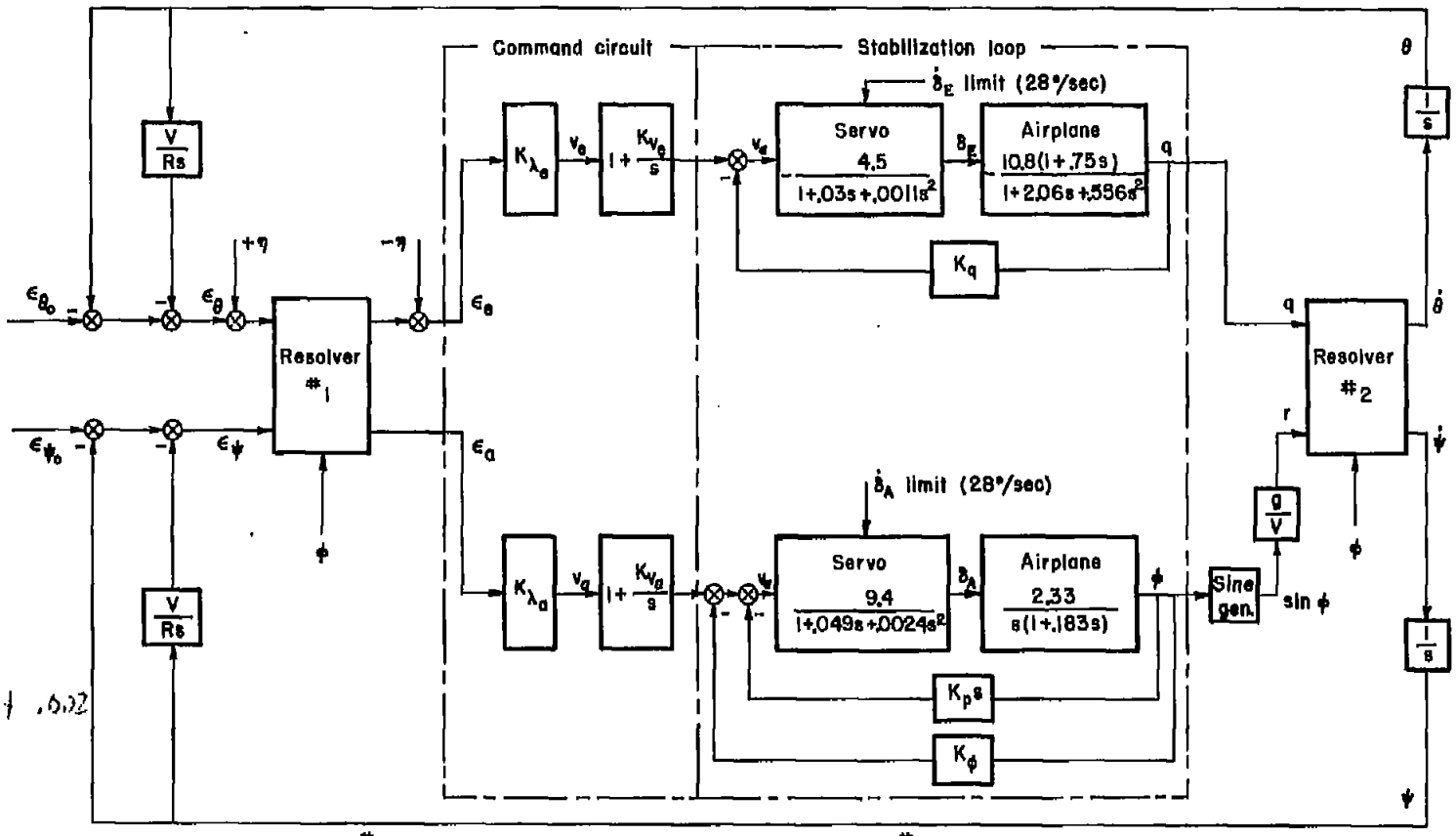

Resolver #1

$$\epsilon_\theta + \eta = \epsilon_\psi \sin\phi + (\epsilon_\theta + \eta)\cos\phi$$
$$\epsilon_a = \epsilon_\psi \cos\phi - (\epsilon_\theta + \eta)\sin\phi$$

Resolver #2

$$\dot{\theta} = q\cos\phi - r\sin\phi$$
$$\dot{\psi} = r\cos\phi + q\sin\phi$$

Perfect rudder servo

Zero sideslip

$$r = \frac{g}{V}\sin\phi$$

Figure 7.- Block diagram of REAC simulation of SB2C-5 automatic control system.

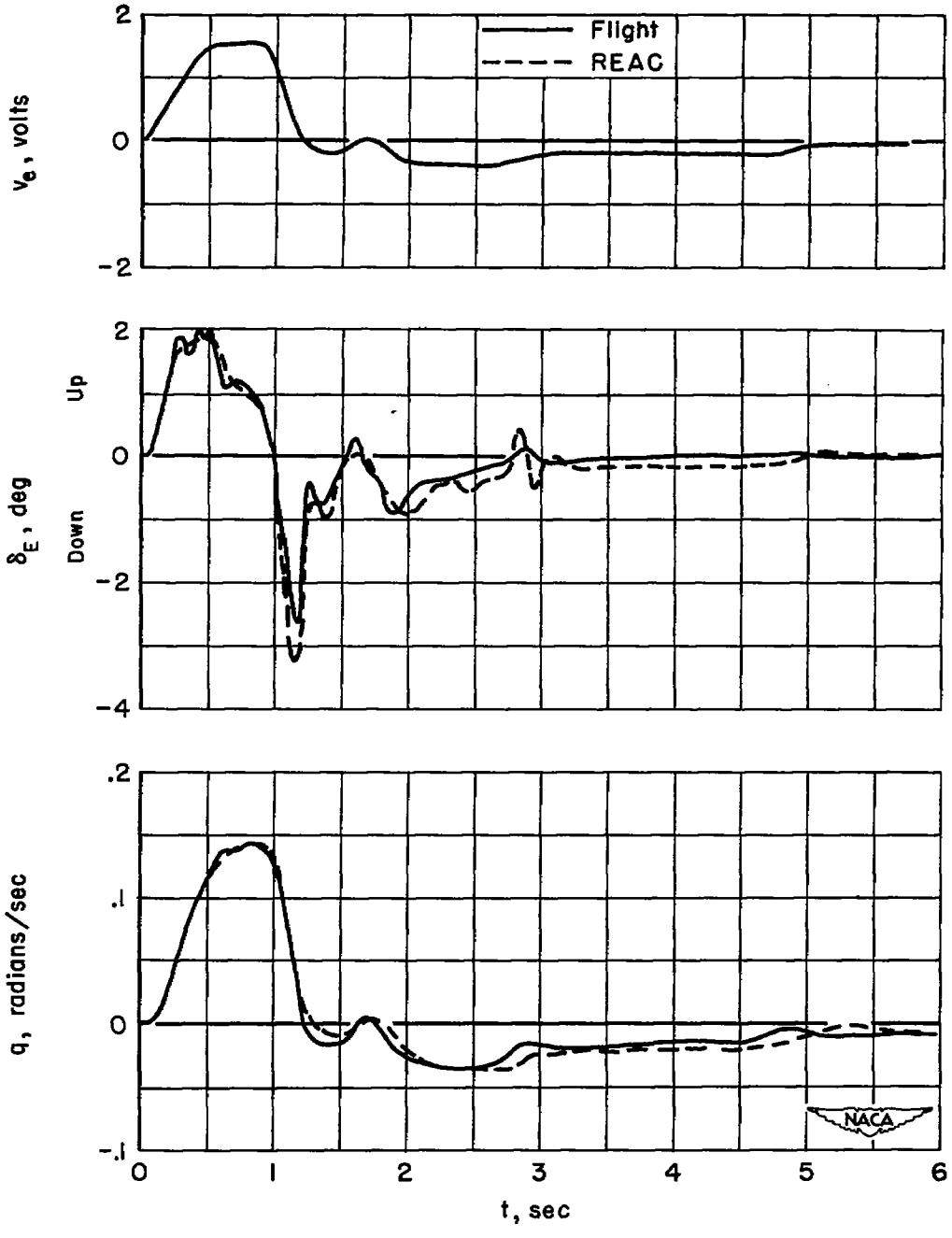

(a) Elevation stabilization loop (c), table I.

Figure 8.— Comparison of interceptor response to a known input as measured in flight and as determined from REAC studies.

[redacted]

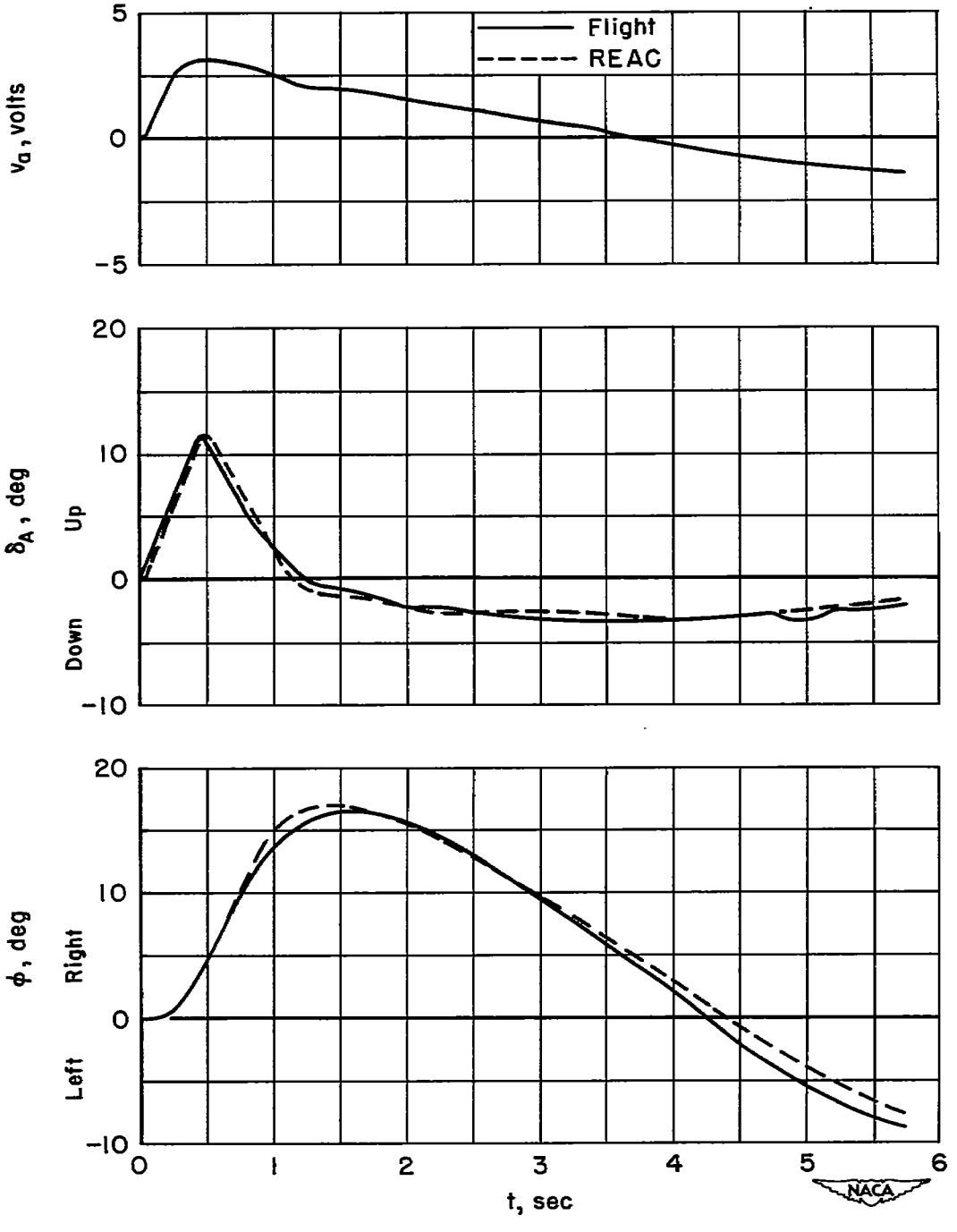

(b) Azimuth stabilization loop (c), table I.

Figure 8.– Concluded.

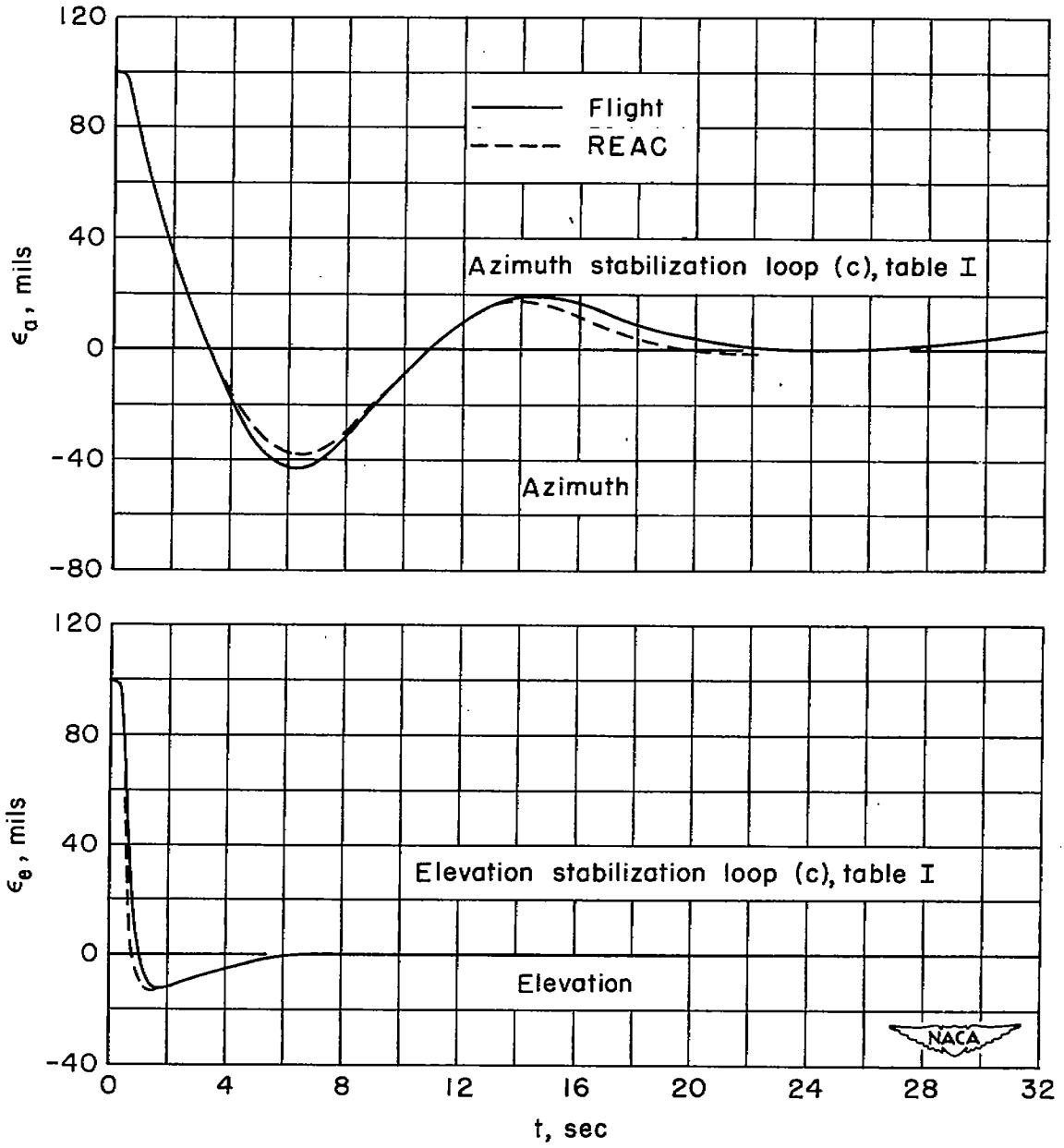

Figure 9.– Comparison of the tracking performance as measured in flight and as determined from REAC studies. Lock-on maneuver from 100-mil initial error; nonmaneuvering target; simple command system.

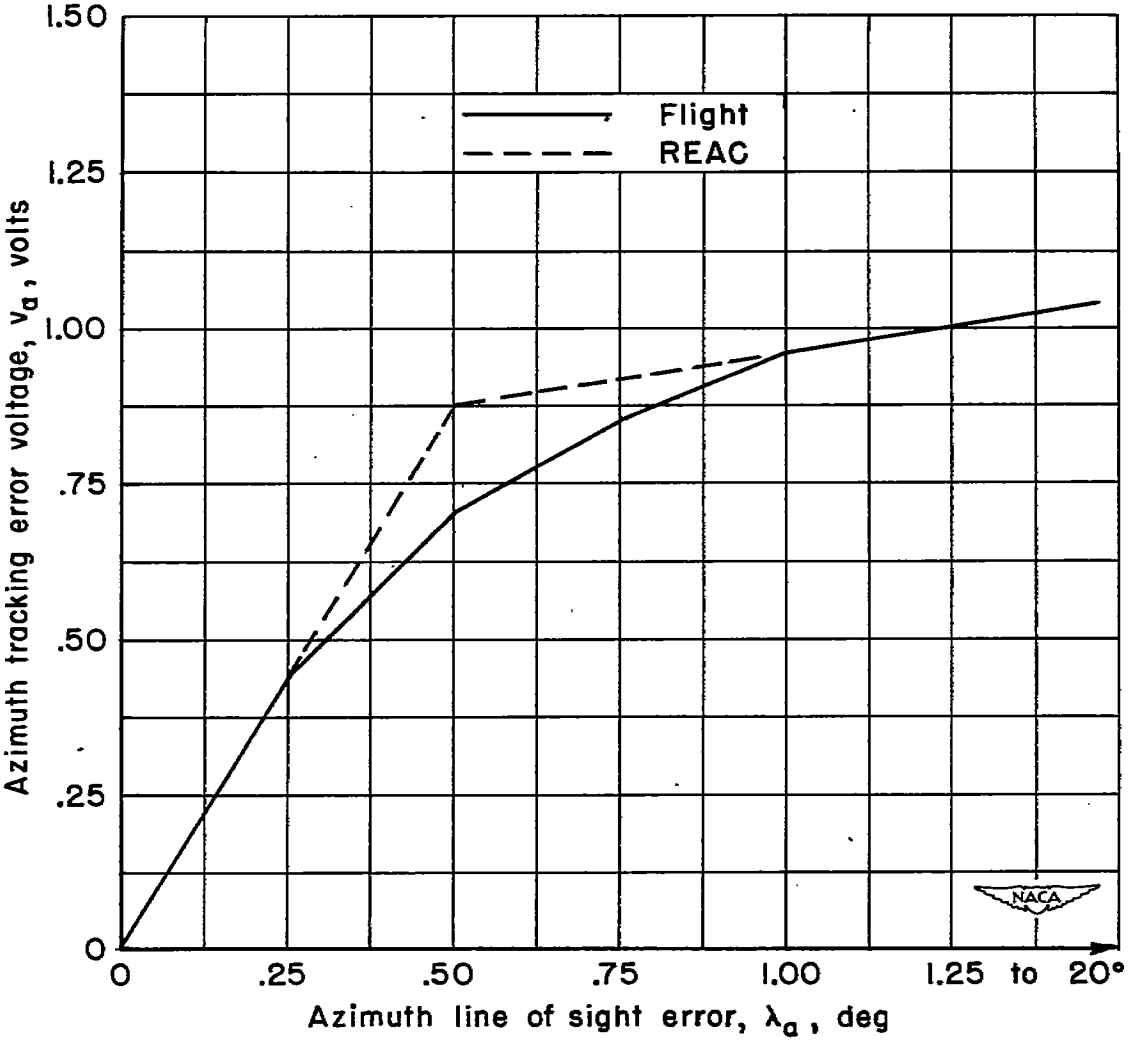

Figure 10.— Azimuth command signal nonlinearity.

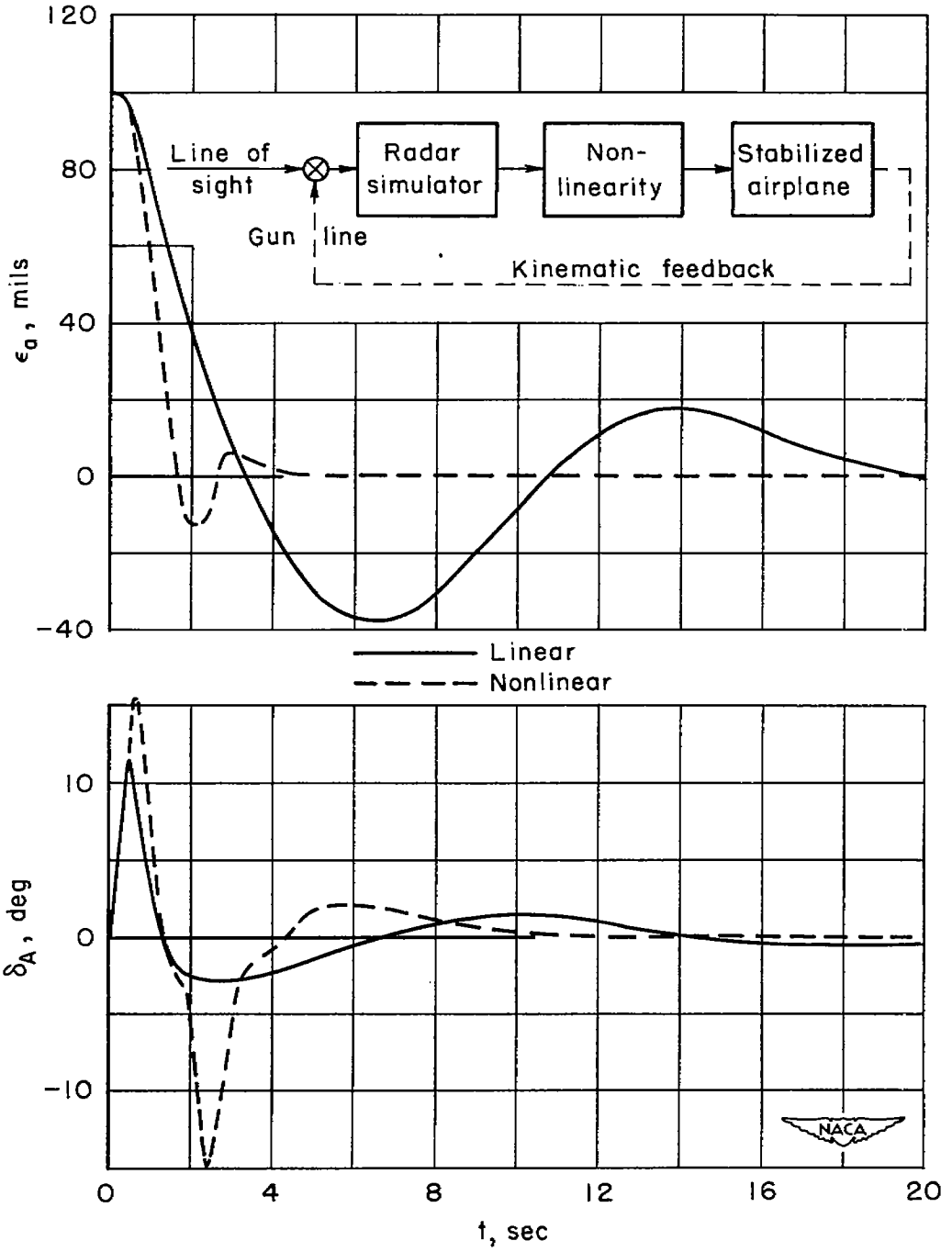

Figure 11.- Comparison of tracking performance with linear and nonlinear command signal gains as indicated by REAC studies.

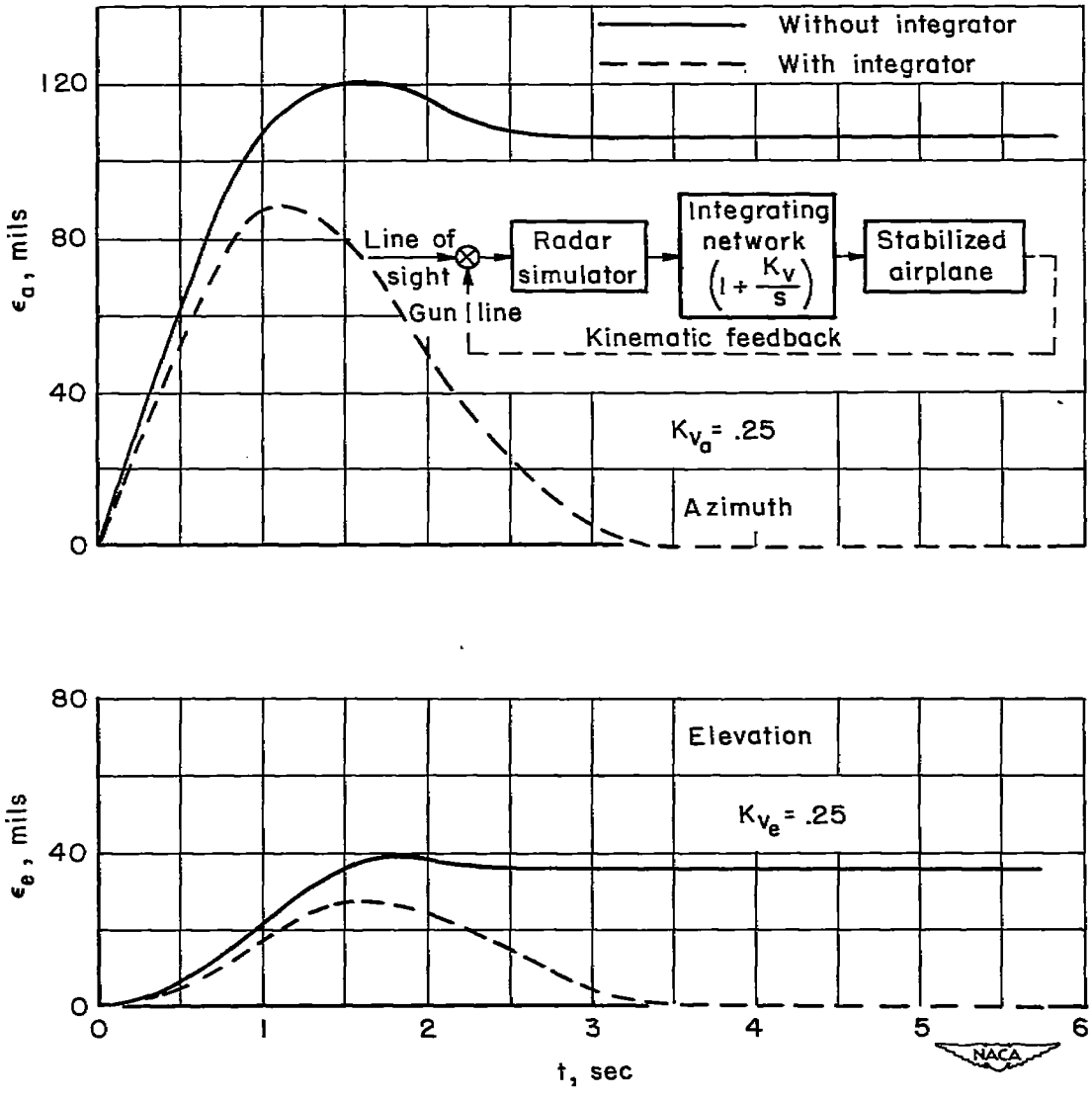

Figure 12.– Effect of integrating networks on the tracking performance in simulated 8° per second steady turns as determined from REAC studies.

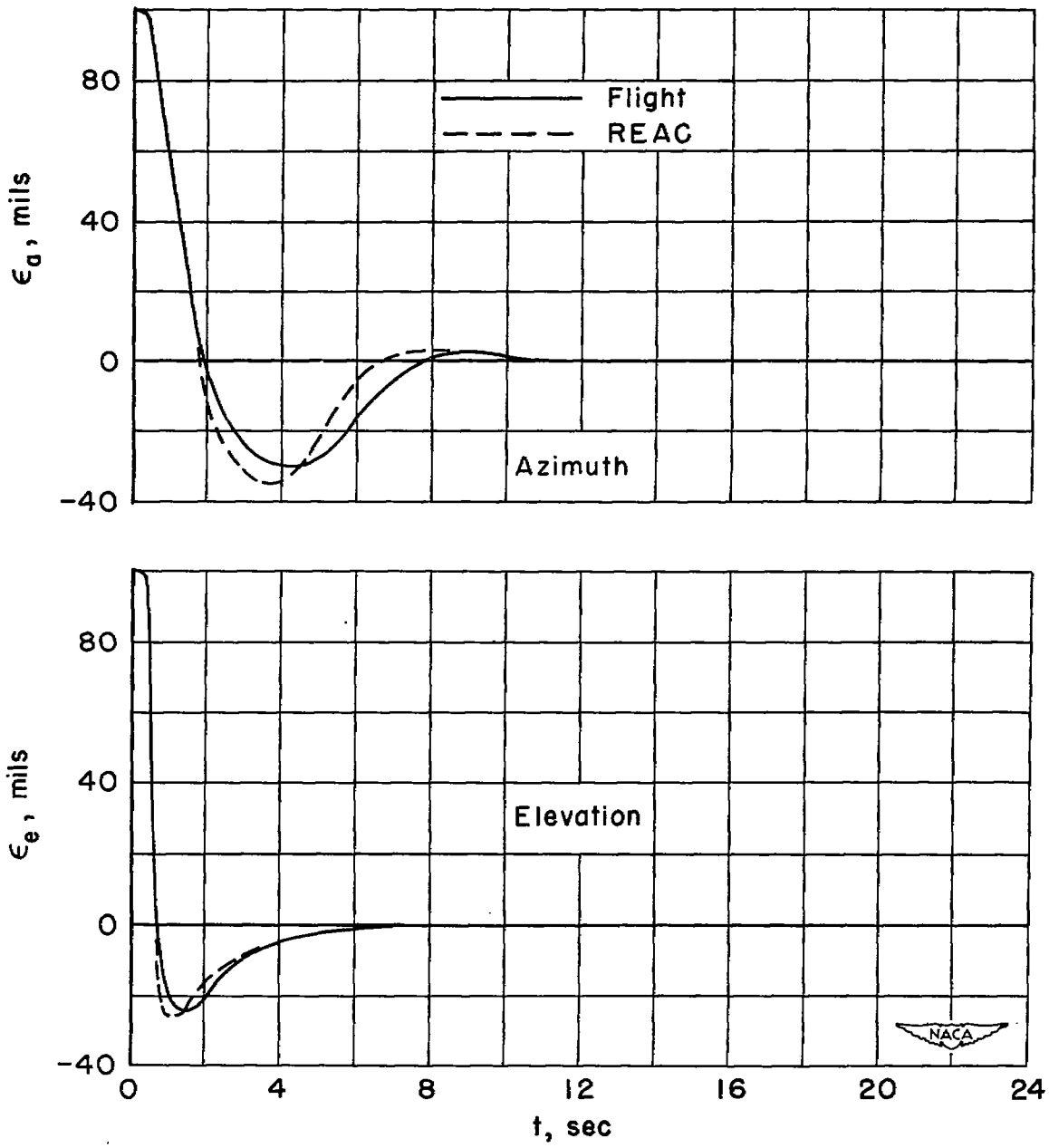

Figure 13.— Comparison of the tracking performance as measured in flight and as determined from REAC studies. Improved command system with azimuth nonlinearity and with azimuth and elevation integrating networks. Lock-on maneuver from 100-mil initial error; nonmaneuvering target.

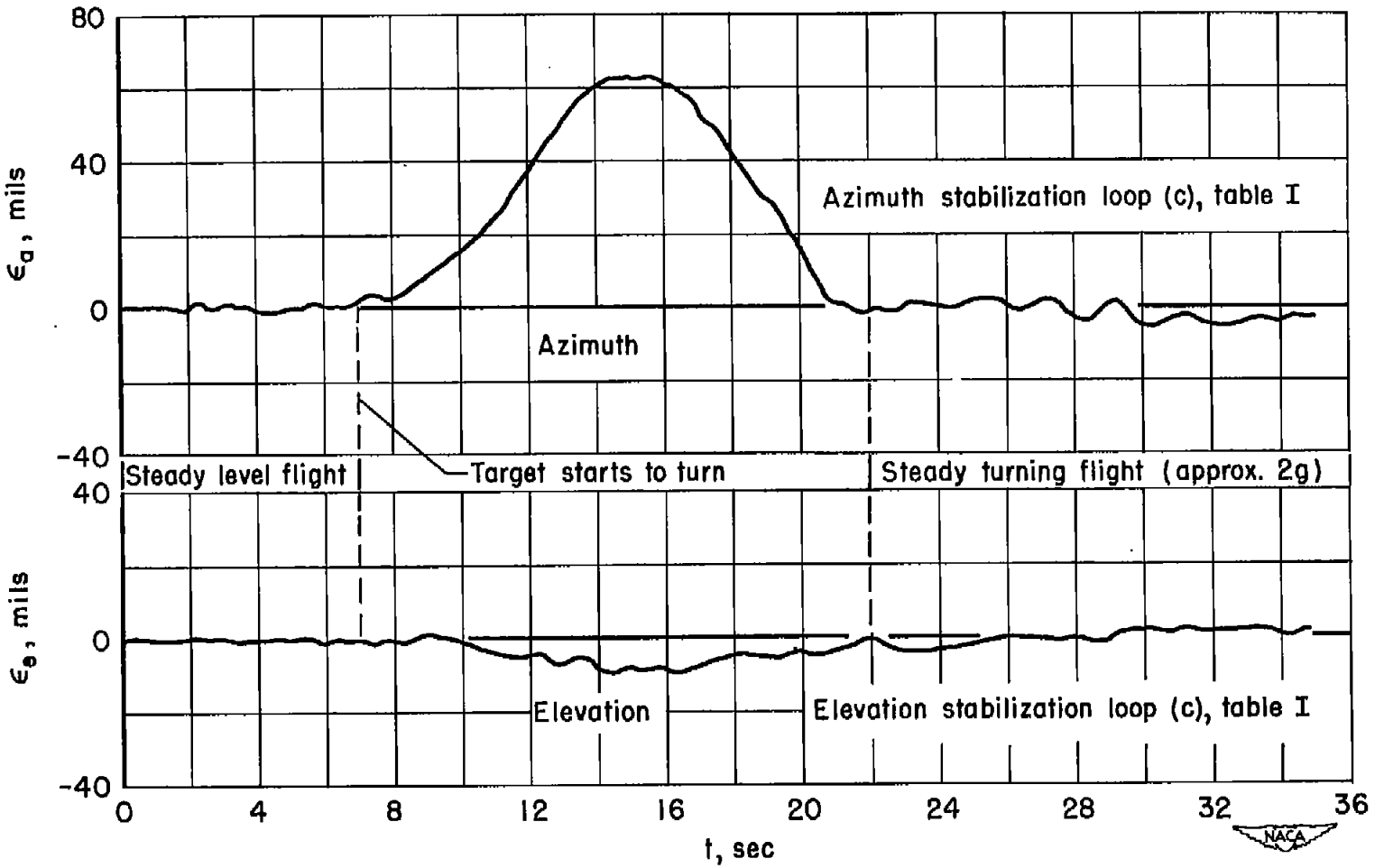

Figure 14.- Typical gun-line wander during the transition between steady level and steady turning flight; automatic control with the improved command system.

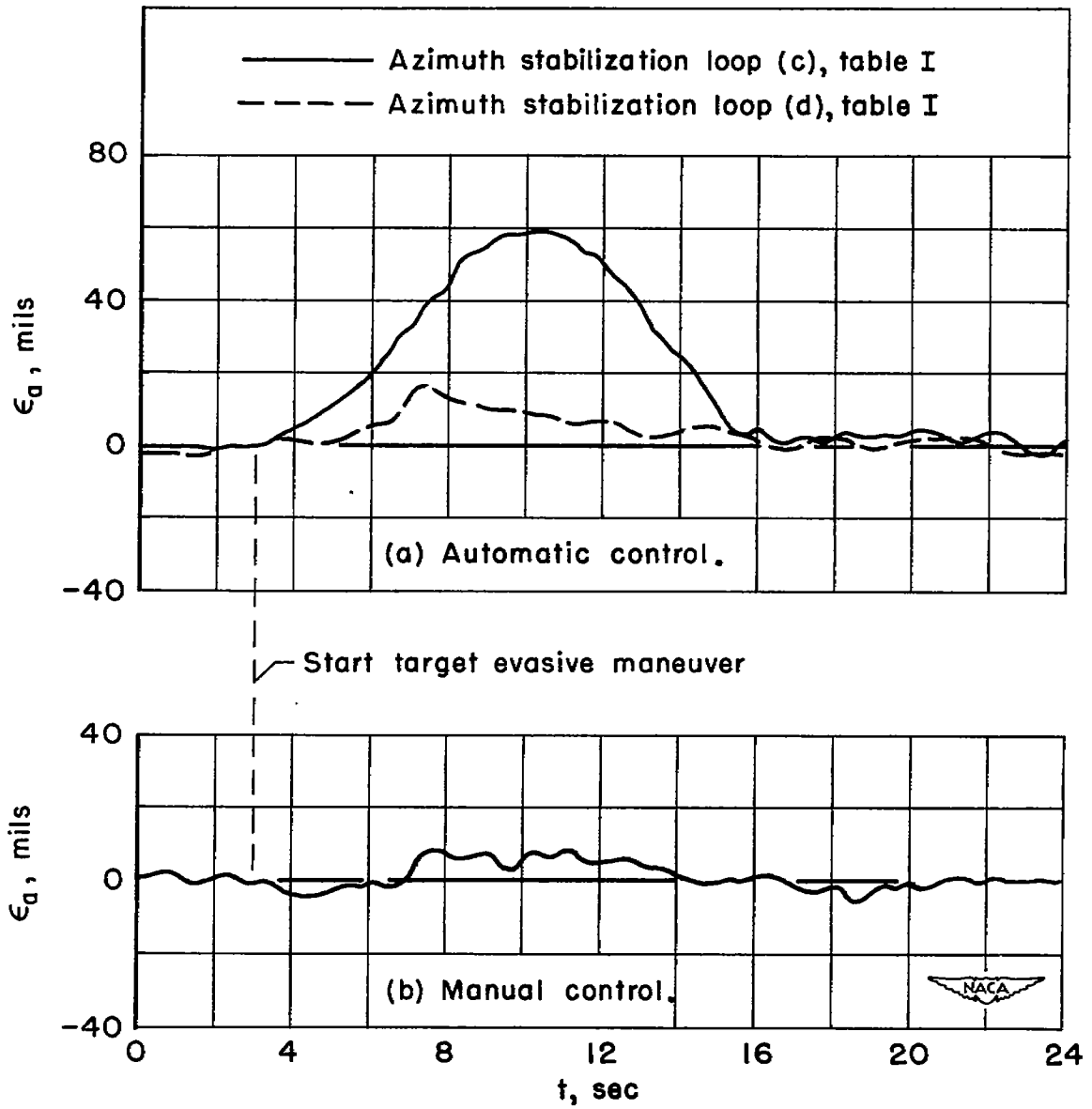

Figure 15.- Typical azimuth gun-line tracking errors obtained in the transition between steady level and steady turning flight under manual control and under automatic control with various stabilization loops and the improved command system.

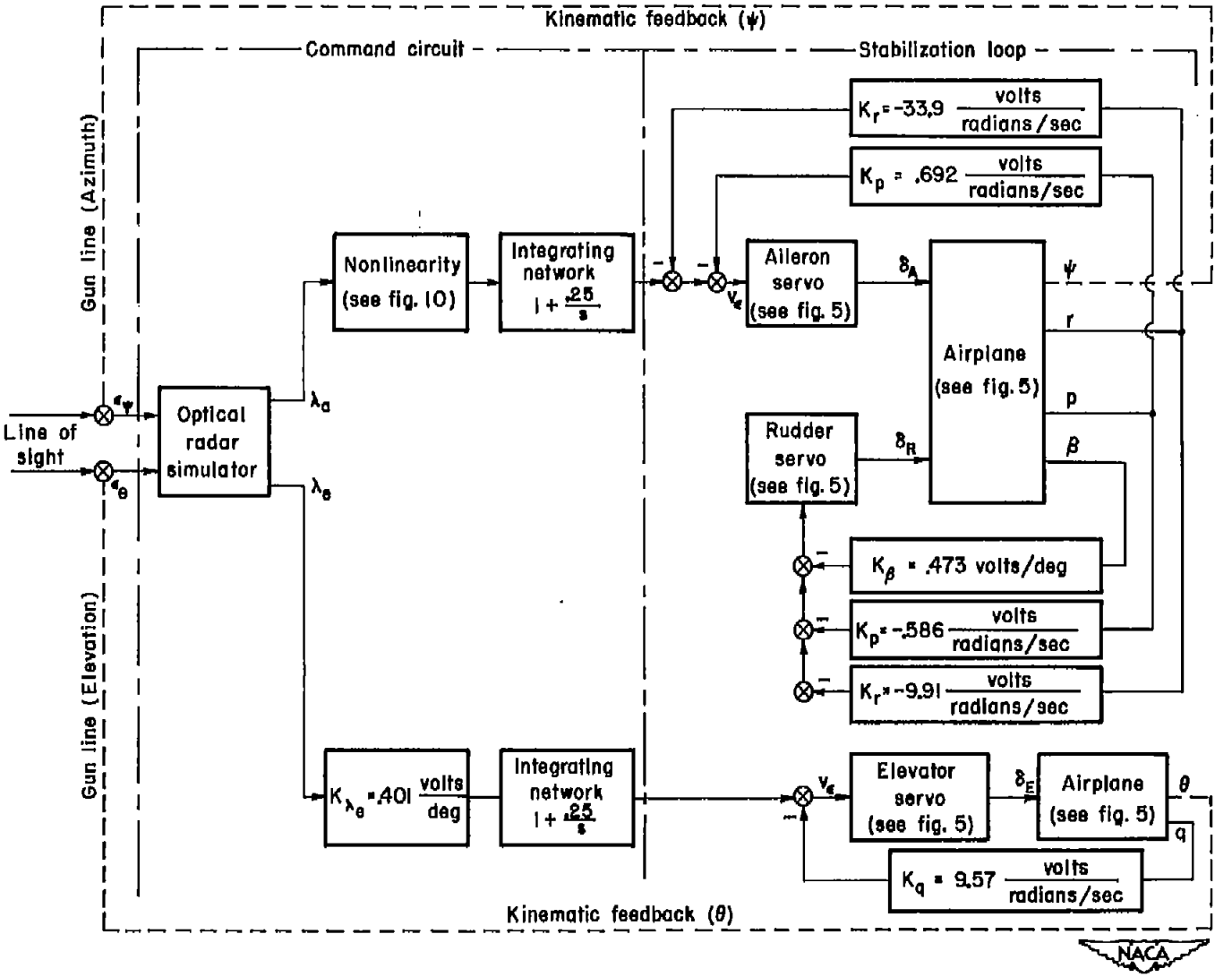

Figure 16.— Block diagram of the SB2C-5 automatic control system selected for evaluation.

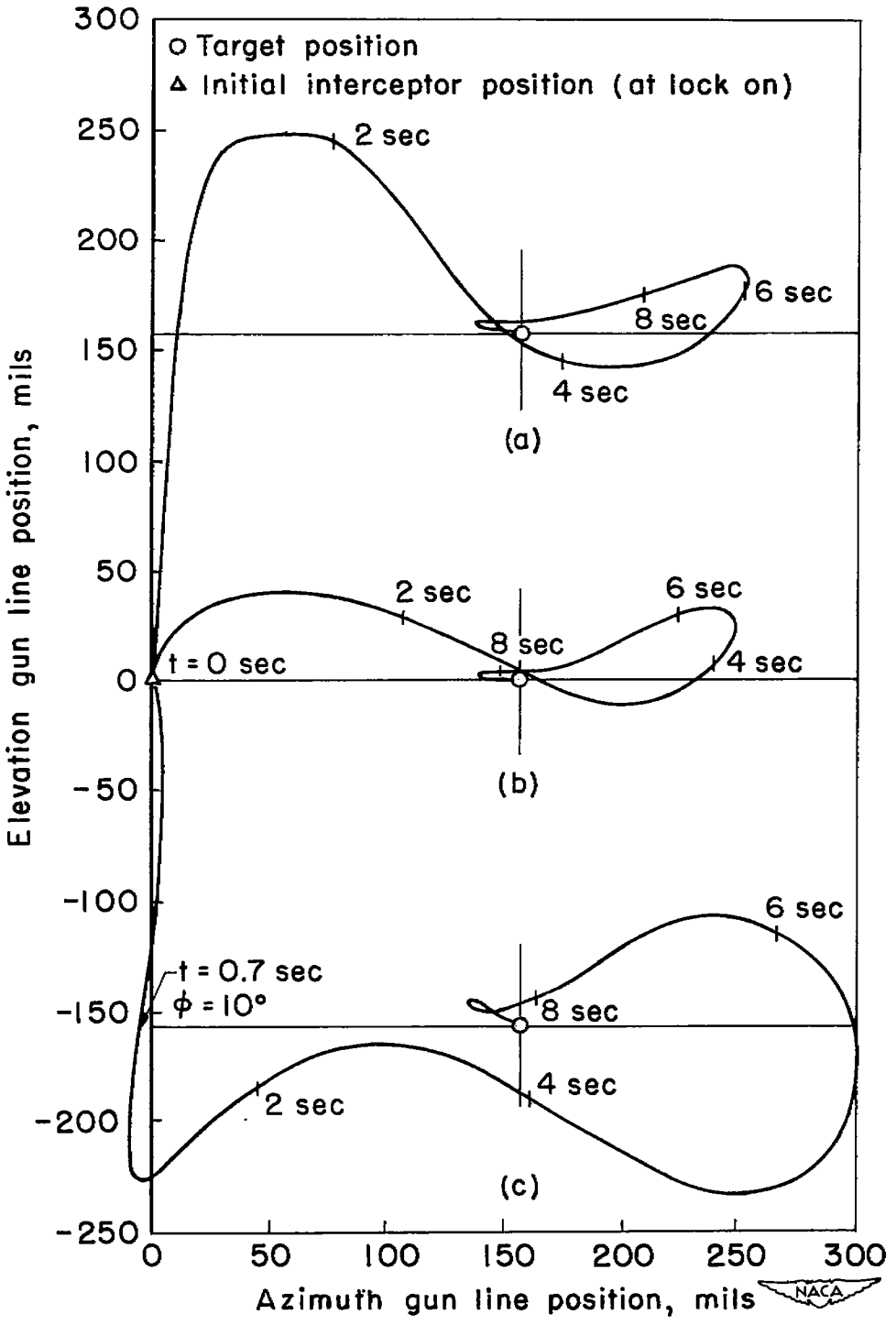

Figure 17.— Effect of combined initial azimuth and elevation errors on the tracking performance of the automatic interceptor as determined from REAC studies.

[redacted]

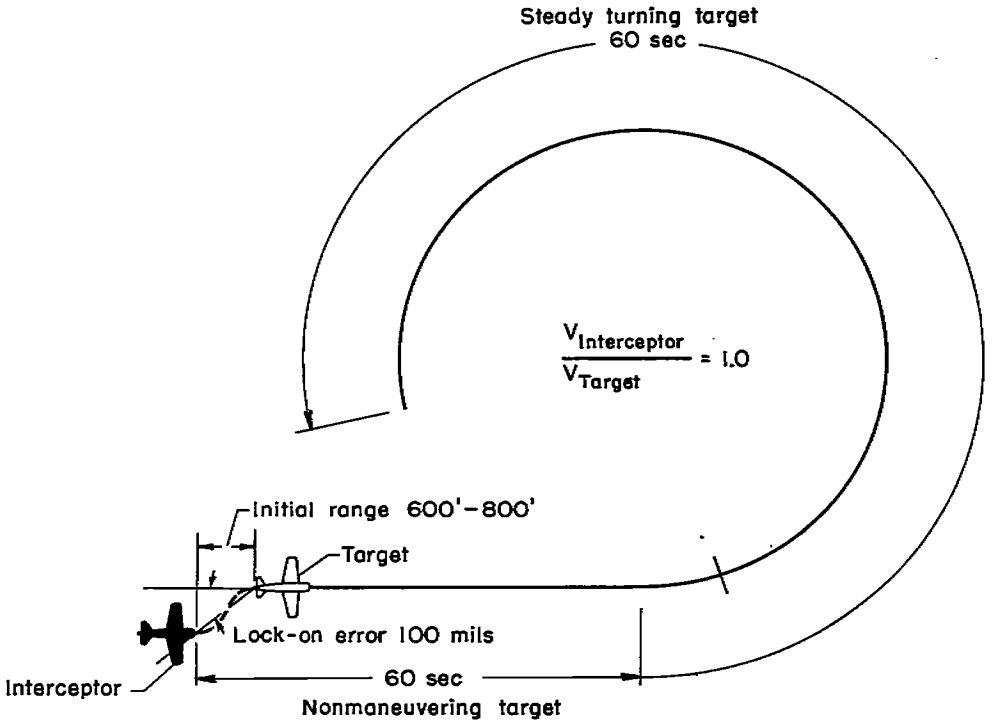

(a) Ames standard gunnery run.

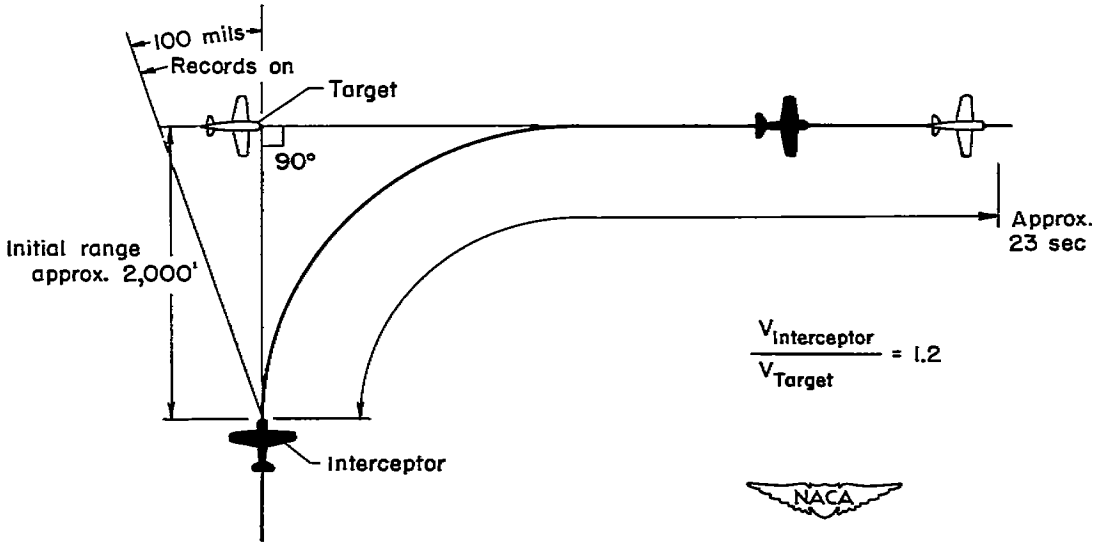

(b) 90° beam attack.

Figure 18.— Plan views of test maneuvers used in this investigation.

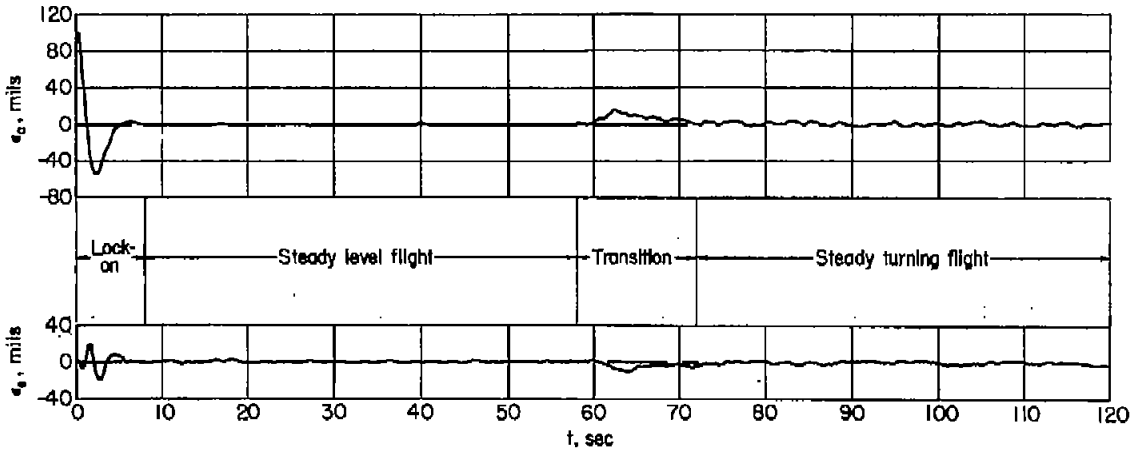

(a) Automatic control.

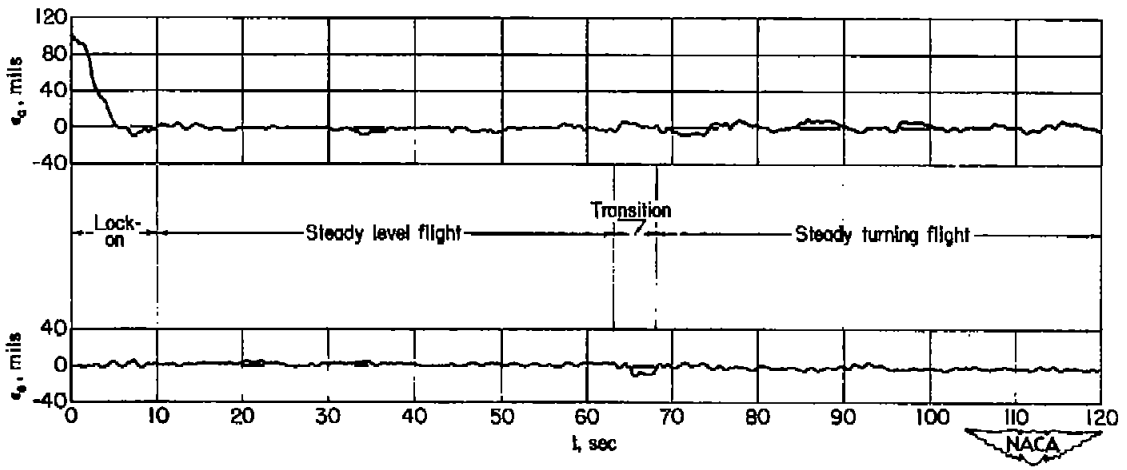

(b) Manual control.

Figure 19.- Comparison of typical tracking performances under automatic control and manual control in Ames standard gunnery runs.

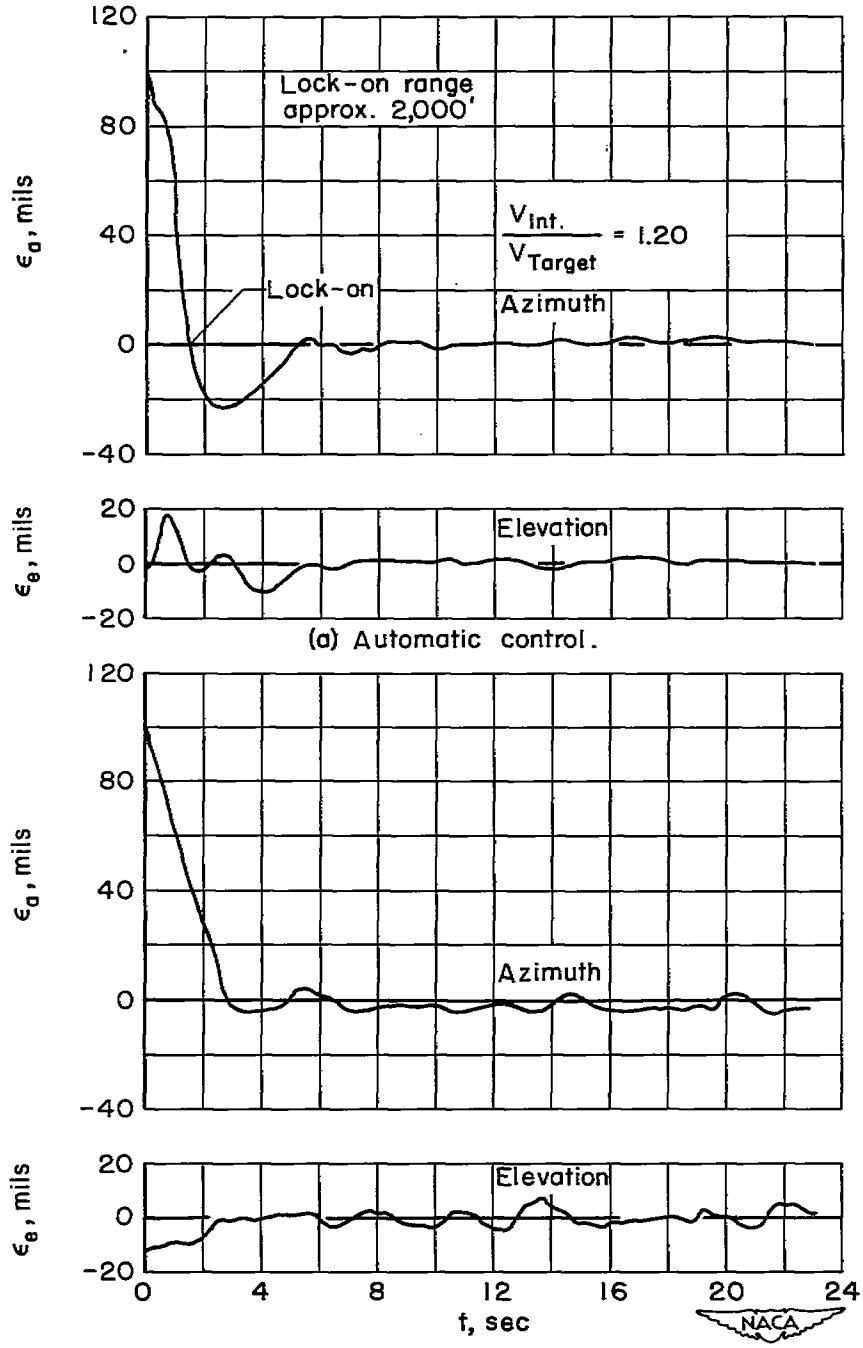

Figure 20.— Comparison of gun-line wander in a typical 90° beam attack under automatic control and under manual control.

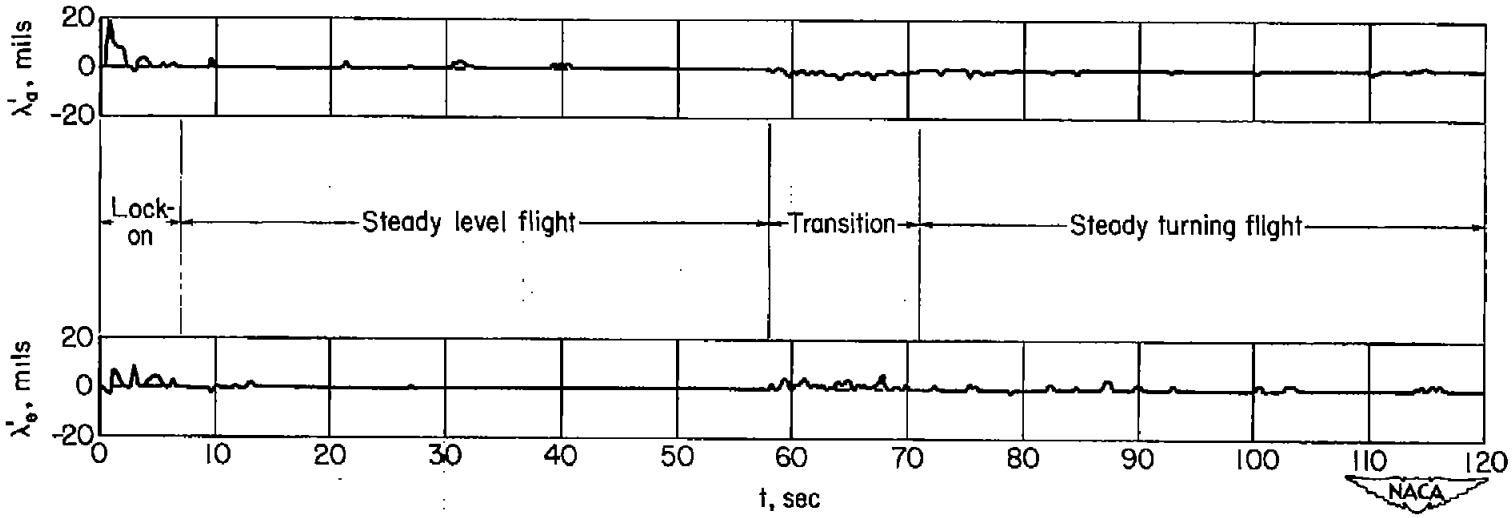

(a) Ames standard gunnery run.

Figure 21.- Typical line-of-sight tracking errors of the simulated radar during an Ames standard gunnery run and a 90° beam attack under automatic control.

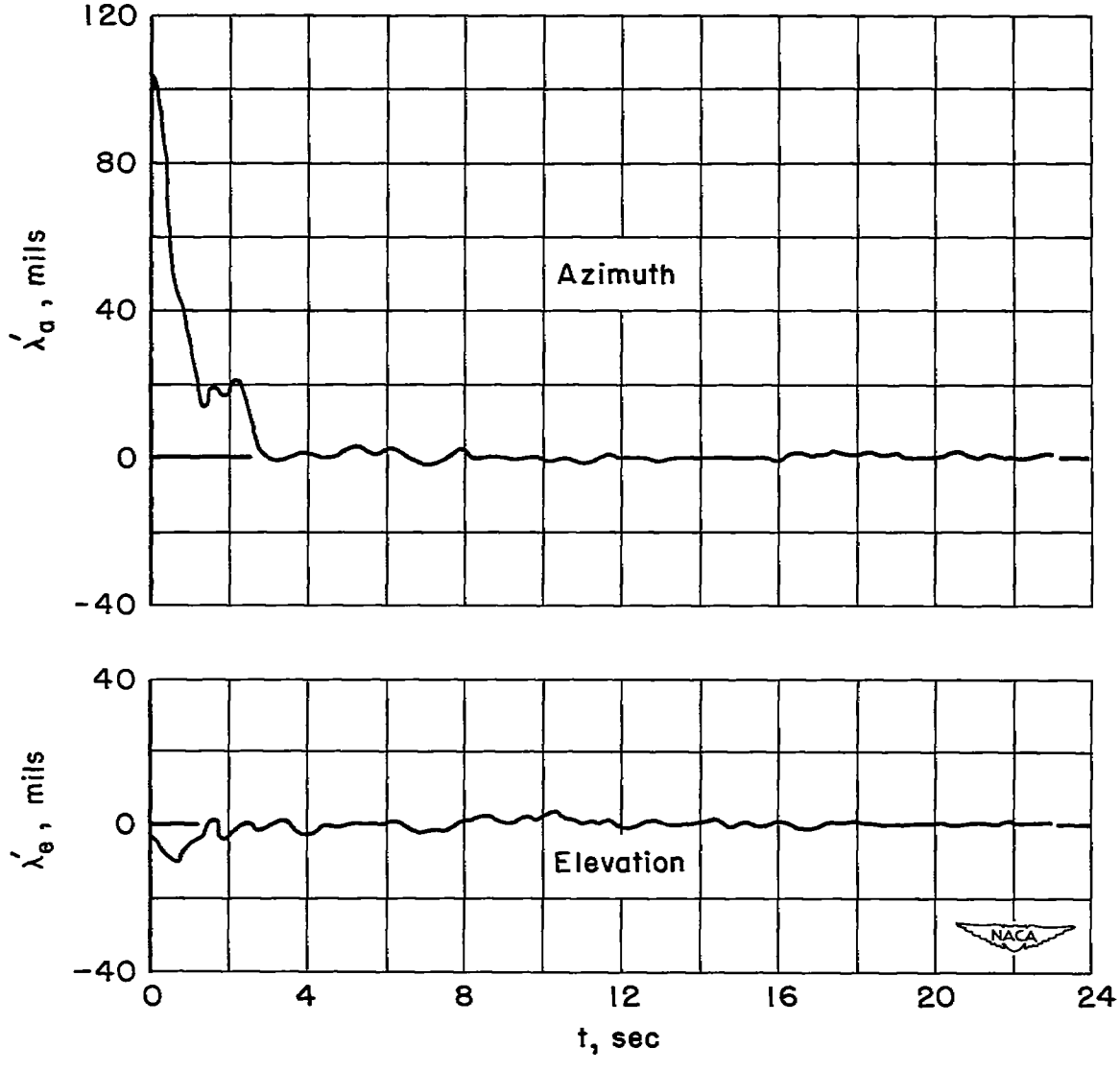

(b) 90° beam attack.

Figure 21.– Concluded

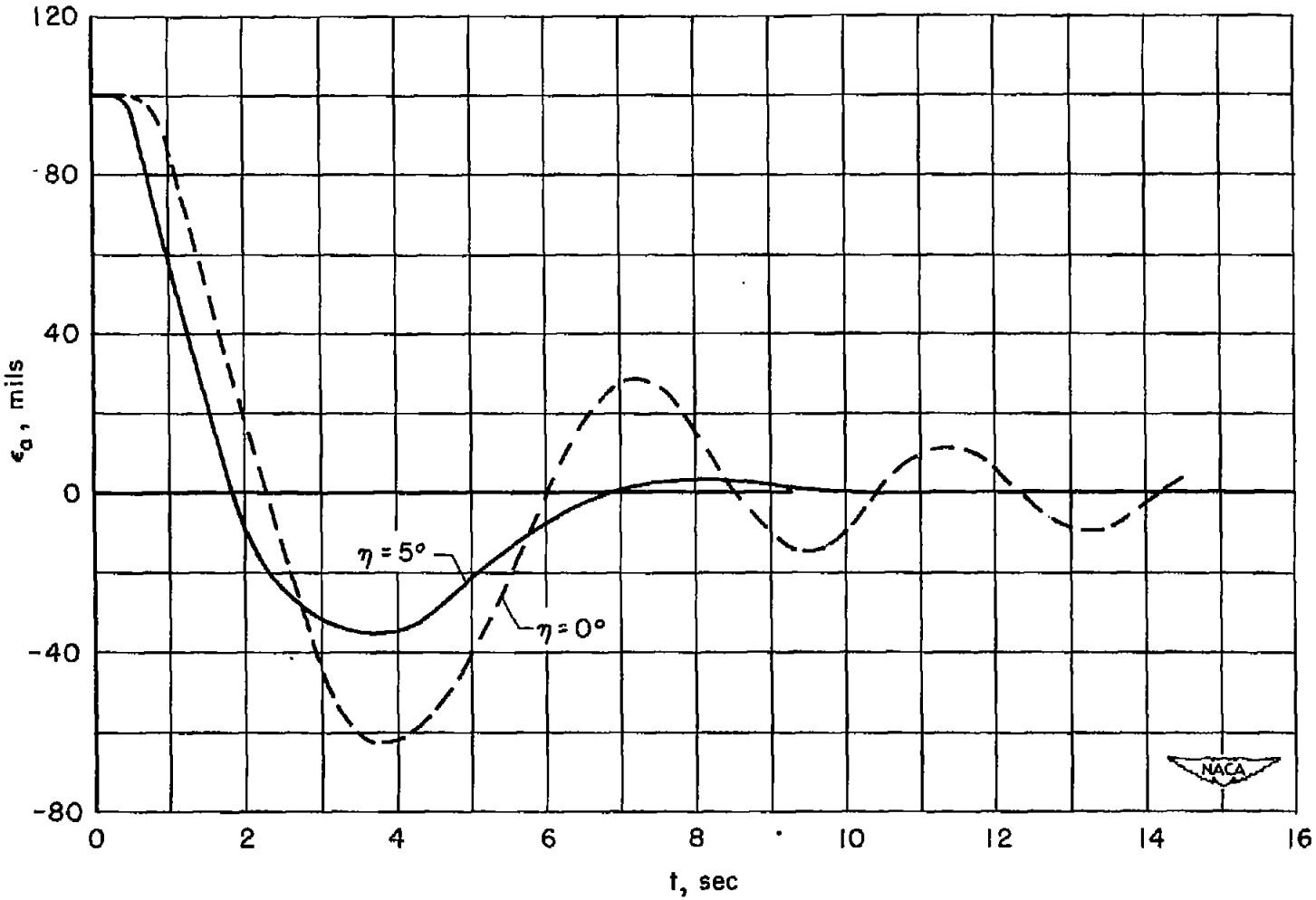

Figure 22.– Effect of inclination of the gun line above the fuselage datum line on the azimuth tracking performance after lock-on on a nonmaneuvering target from a 100-mil initial error as determined from REAC studies.

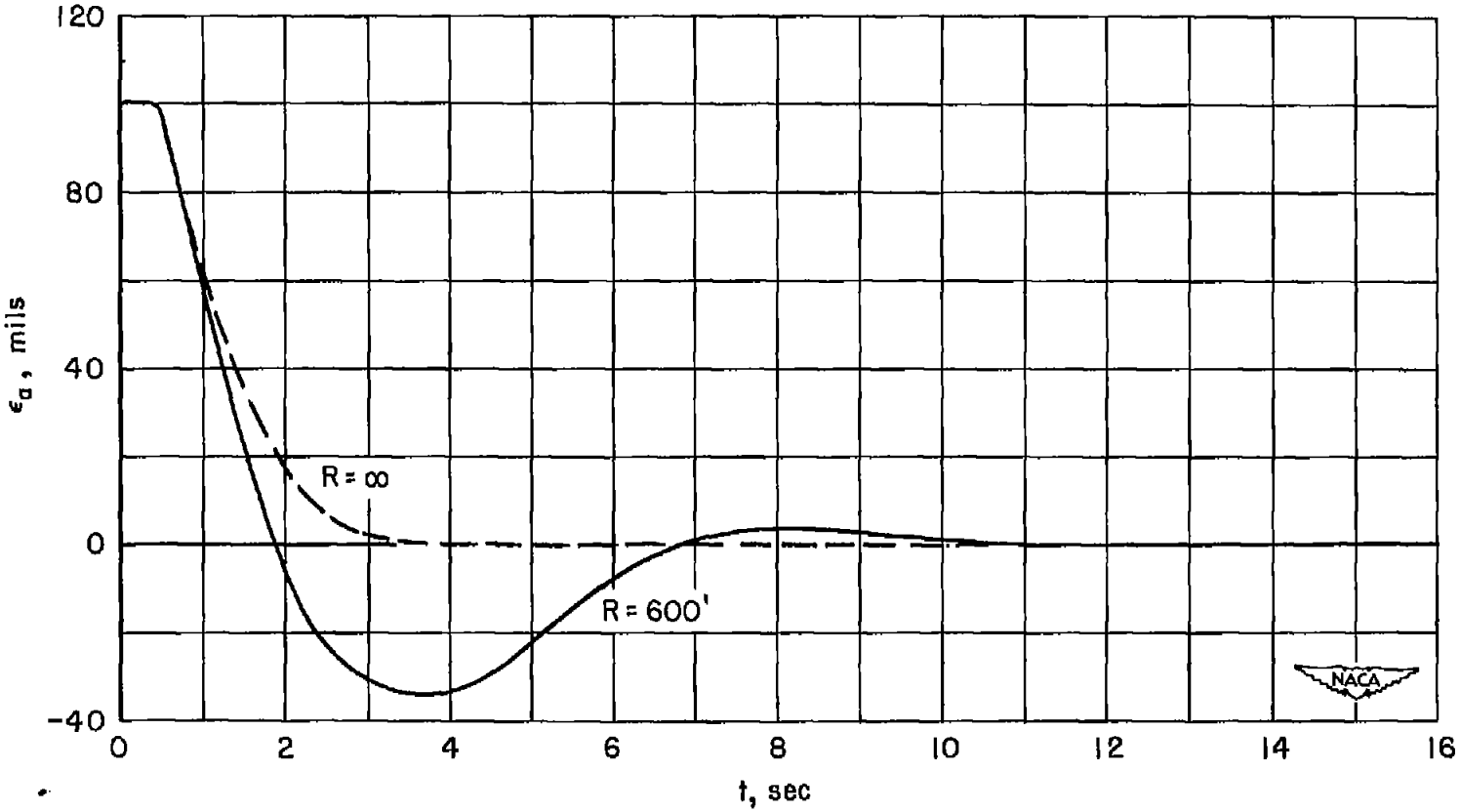

Figure 23.– Effect of range on the azimuth tracking performance after lock-on from a 100-mil initial error on a nonmaneuvering target as determined from REAC studies.